JOC The Journal of Organic Chemistry

Article

Bridge Chlorinated Bicyclo[1.1.1]pentane-1,3-dicarboxylic Acids

Ji#í Kaleta, Igor Ron#evi#, Ivana Cisarova, Martin Dracinsky, Veronika Šolínová, Vaclav Kasicka, and Josef Michl

J. Org. Chem., **Just Accepted Manuscript** • Publication Date (Web): 24 Jan 2019

Just Accepted

ACS Publications

is published by the American Chemical Society. 1155 Sixteenth Street N.W., Washington, DC 20036

Bridge Chlorinated Bicyclo[1.1.1]pentane-1,3-dicarboxylic Acids

Jiří Kaleta,[a,b]* Igor Rončević,[a] Ivana Císařová,[c] Martin Dračínský,[a] Veronika Šolínová,[a] Václav Kašička,[a] and Josef Michl[a,b]

[a] *Institute of Organic Chemistry and Biochemistry of the Czech Academy of Sciences, Flemingovo nám. 2, 166 10 Prague 6, Czech Republic.*
[b] *Department of Chemistry, University of Colorado, Boulder, CO 80309-0215, United States.*
[c] *Department of Inorganic Chemistry, Faculty of Science, Charles University in Prague, Hlavova 2030, 12840 Prague 2, Czech Republic.*

TOC Graphic

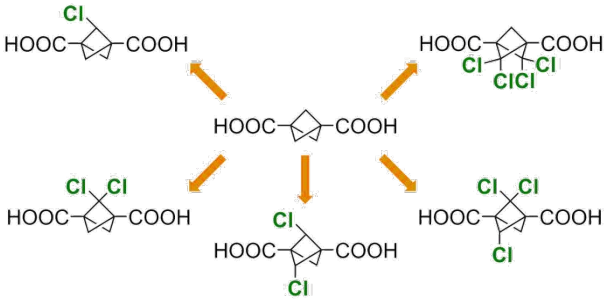

ABSTRACT

Radical chlorination of bicyclo[1.1.1]pentane-1,3-dicarboxylic acid is highly selective and up to four chlorine atoms can be introduced relatively easily without damage to the strained bicyclic cage. Combined with hydrodechlorination with TMS_3SiH, direct chlorination provides access to five of the 15 possible chlorinated diacids. Their configuration has been established by X-ray diffraction. Their pK_a values have been measured by capillary electrophoresis and calculated at the B3LYP-D3BJ/6-311+G(d,p)-level. The results are in good agreement and reflect the expected trend, from 2.78 ± 0.08 and 4.14 ± 0.10 in the parent to 1.07 ± 0.03 and 2.31 ± 0.03 in the tetrachlorinated diacid). Strain energy relative to the parent diacid was calculated for all 15 chlorinated diacids and shows a dramatic increase with successive chlorination, due to non-bonded Cl - Cl repulsions.

INTRODUCTION

The highly strained yet remarkably stable bicyclo[1.1.1]pentane evolved during the past few decades from a laboratory curiosity to an important player in organic synthesis.[1,2,3,4] Hundreds of the relatively easily accessible 1,3- (bridgehead) substituted derivatives have been described and are essential components of numerous systems, from molecular devices[5,6,7,8,9,10,11,12,13,14,15] to biologically active structures.[16,17,18,19,20,21,22,23]

Only a few examples of bridge-substituted derivatives are known, almost all of them either with a halogen or a carbon-based substituent. The introduction of the latter requires a demanding multistep synthesis of the cage, often from complex precursors.[24,25,26] The ease of halogenation reflects the reactivity of the halogen. Direct iodination and bromination[27] do not take place. Bridge-iodinated derivatives are not known and the only brominated ones are geminal dibromides, made by addition of dibromocarbene to substituted bicyclo[1.1.0]butanes.[28] Such addition was also used to prepare the first 2,2-dichloro analogues.[28,29,30] It was later discovered that this structure is easily accessible by direct chlorination of 1,3-disubstitued bicyclo[1.1.1]pentanes, and that subsequent reduction with *n*-

Bu_3SnH affords the monochlorinated product.[27] Direct fluorination under mild reaction conditions is unselective and yielded 14 of the 15 possible bridge-fluorinated derivatives, separated by preparative gas chromatography.[31] Exhaustive fluorination followed by repeated crystallization afforded penta- and hexafluoro derivatives in synthetically useful yields.[32]

Since there is an obvious need to extend the library of laterally substituted derivatives, which might also serve as precursors to bridge-bridge bond containing polycyclic cages,[33] we decided to explore the scope of direct chlorination of the parent bicyclo[1.1.1]pentane-1,3-dicarboxylic acid (**0**) in the form of its dichloride. We improved the previously published27 syntheses of mono- and dichlorinated diacids and found reaction conditions for three new diacids with up to four chlorine atoms (Chart 1). Purification requires only simple column chromatography and all five products are in principle accessible in multigram quantities. We were unable to introduce five or six chlorine atoms. All five diacids have been fully characterized, their pK_a values measured and compared with calculated numbers, and single-crystal X-ray structures of four chlorinated dicarboxylic acids and three esters have been solved. The relative strain energies for all possible chlorinated diacids were calculated.

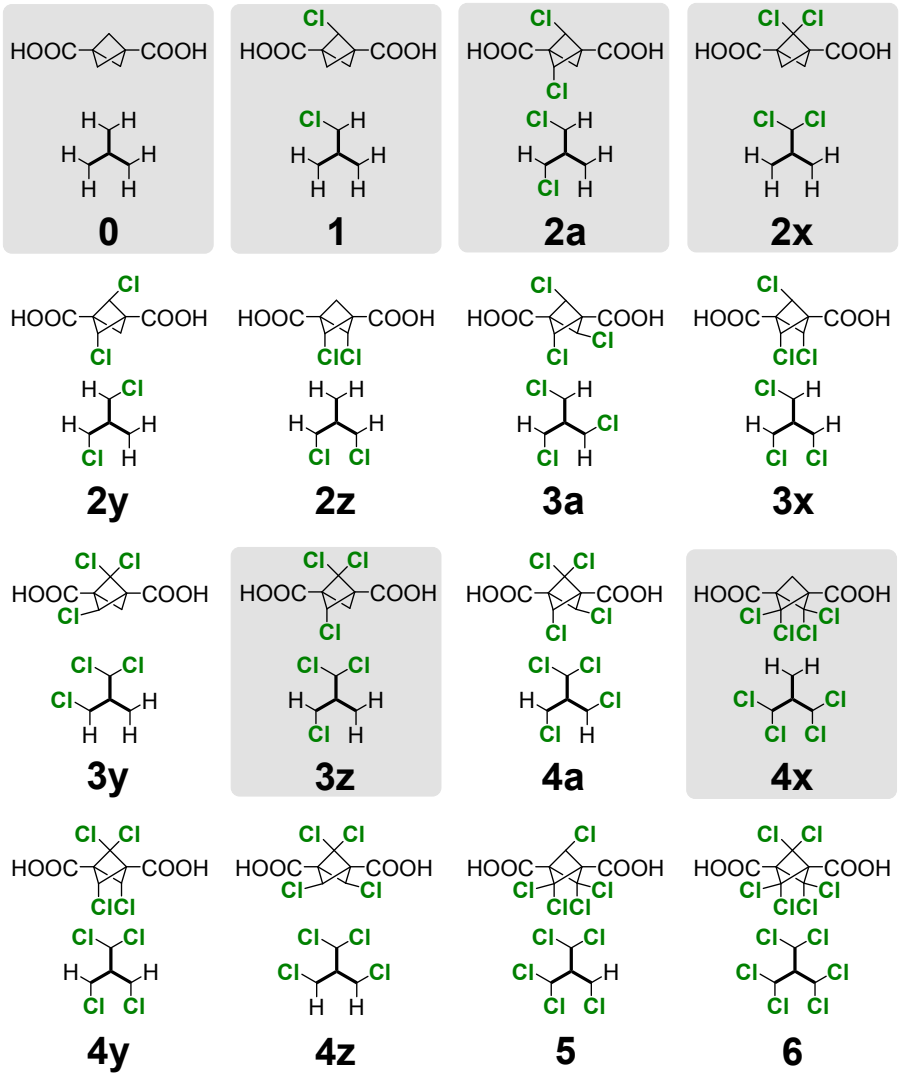

Chart 1. Chemical structures of parent (**0**) and chlorinated (**1** - **6**) diacids. The labels follow the pattern introduced earlier[31] for the fluorinated

analogues. Previously known and newly synthesized compounds are highlighted in gray.

RESULTS

Synthesis. The parent diacid **0** was converted to the dichloride **7** (Scheme 1)[34] and gently chlorinated in CCl_4 saturated with Cl_2 at 0 - 5 °C under irradiation with visible light to generate the highly reactive monochlorinated double acid chloride that was immediately further chlorinated and is related to **8** by methanolysis. Quenching with MeOH afforded **9x** and **10z** in a ~7:1 ratio (Scheme 1A), easily separable by column chromatography. ^{1}H NMR analysis of the crude reaction mixture revealed only traces of **8**. When the chlorination was performed at 60 - 65 °C, the ratio of products **9x** and **10z** changed to 1:7 (Scheme 1B). Subsequent chlorination of the double acid dichloride of **10z** leads to formation of **11x**, but under these conditions only traces were detected by ^{1}H NMR in the crude reaction mixture.

Radical chlorination of **7** under harsher reaction conditions employing liquid chlorine at 50 °C in a high-pressure Schlenk flask followed by methanolysis afforded **11x** almost quantitatively, based on ^{1}H NMR of the crude reaction mixture. It was isolated in 74% yield by column chromatography (Scheme 1C).

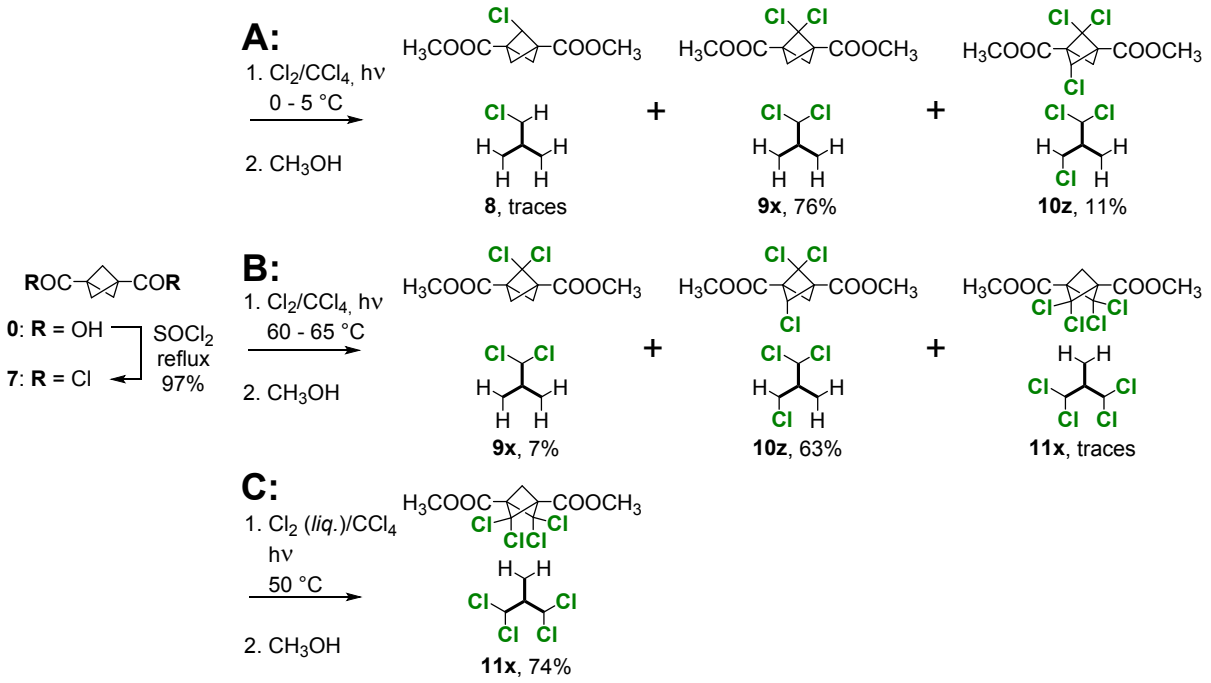

Scheme 1. Radical chlorination of **0**.

Reduction of **9x** with TMS_3SiH in refluxing benzene in the presence of AIBN provided **8** in nearly quantitative yield (Scheme 2).20 Under the same reaction conditions **10z** gave **9a** quantitatively and in excellent isolated yield. The other dichlorinated isomer was not detected. Surprisingly, the reduction of **11x** led to complete destruction of the cage and only traces of **10z** were observed in the ^{1}H NMR spectrum of the crude reaction mixture (Scheme 2).

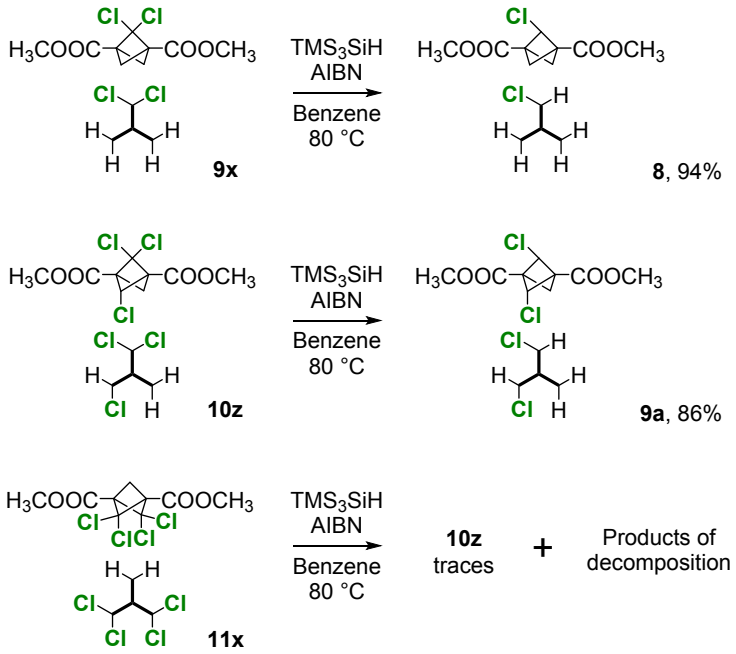

Scheme 2. Reduction using TMS_3SiH.

Carboxylic acids **1**, **2a**, **2x**, **3z**, and **4x** were liberated from the corresponding methyl esters **8**, **9a**, **9x**, **10z**, and **11x** with LiOH in aqueous THF (Scheme 3) and the products were isolated in 87 - 97% yields.

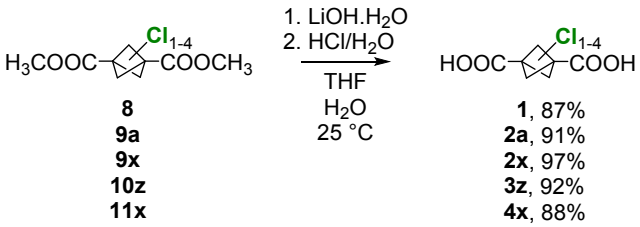

Scheme 3. Liberation of carboxylic acids **1**, **2a**, **2x**, **3z**, and **4x** from methyl esters.

In contrast, basic hydrolysis of **9x** under heterogenous conditions gave not only the expected **2x** but also the cyclobutene derivative **12** (Scheme 4), which was characterized as the diester **13** after quantitative esterification with ethereal diazomethane (Scheme 4).

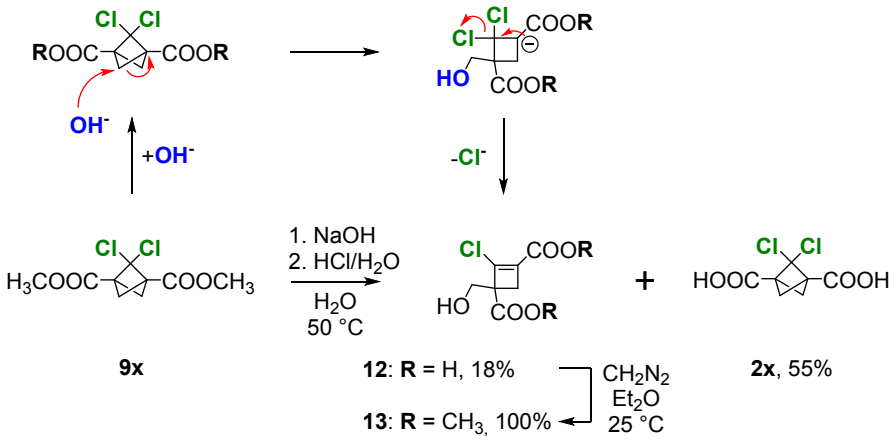

Scheme 4. Heterogeneous basic hydrolysis of **9x** and proposed formation mechanism of a cyclobutene.

X-ray Crystallography. We were able to grow high quality single crystals of four diacids **1**, **2x**, **3z** and **4x** from acetone. Compound **2a** crystallized from the same solvent as well, but the crystals decomposed at a low temperature. High temperature data provided a highly disordered structure whose satisfactory solution could not be reached. Crystals of the esters **9a**, **9x**, and **10z** were obtained by slow crystallization from CH_2Cl_2. Compound **8** is an oil at ambient conditions. All attempts to grow single crystals of **11x** failed, because it usually remained oily and slowly solidified once solvents evaporated, or formed an emulsion during diffusion experiments. The crystallographic parameters are summarized in Table S1 in the Supporting Information. Almost all the compounds formed monoclinic crystals and only the crystals of **3z** and **9a** were triclinic.

The X-ray diffraction data established the positions of the Cl atoms unambiguously. Figure 1 shows ORTEP visualizations of selected chlorinated representatives: acids **1**, **2x**, **3z**, and **4x**, and ester **9a**. The chlorine atoms were in all cases located in the plane defined by the three methylene carbons.

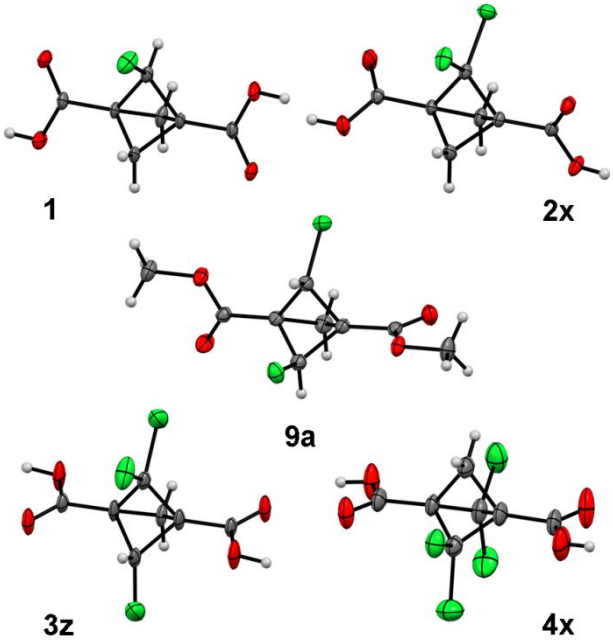

Figure 1. ORTEP visualizations of carboxylic acids **1**, **2x**, **3z**, and **4x** and ester **9a**, representative of all available isomers of chlorinated bicyclo[1.1.1]pentane cages. Atom labeling: chlorine = green, oxygen = red, carbon = gray, and hydrogen = white. Thermal ellipsoids are shown with 50% probability.

Selected interatomic distances are presented in Table 1 (Figure 2). The length of skeletal C-C bonds connecting the bridgehead C atoms with those of the chlorinated methylene bridges is almost constant in the relatively narrow region 154.2 - 155.9 pm. The C-C bonds connecting the bridgehead atoms with CH_2 bridge carbon atoms exhibit a clear trend. Every attached chlorine atom causes a slight elongation of this bond, from the original 155.3 pm in **1** to 157.4 pm in **4x**. The length of the exocyclic C_1-C_6 and C_3-C_7 bonds is

almost constant at 149.1-150.1 pm. In contrast, the inter-bridgehead distance $C_1 \bullet\bullet\bullet C_3$ increases with the number of Cl atoms attached to the bicyclic skeleton, from 187.1 ppm in **1** to 190.3 ppm in **4x**. Thus, each additional chlorine atom attached to the cage increases the inter-bridgehead distance by ~1.1 pm. As expected, the C=O bonds are slightly shorter in methyl esters (119.5 - 120.5 pm) than in carboxylic acids (121.2 - 124.5 pm). The opposite trend is observed for C-OR bonds, which are shorter in carboxylic acids (125.7 - 130.9 pm) and longer in esters (131.7 - 132.9 pm). The C-Cl bonds are 175.5 - 178.2 pm long. A trend in the length of the C-Cl bonds was found in **4x**: C_1-Cl_1 and C_2-Cl_4 are significantly longer (177.8 - 178.2 ppm) than C_1-Cl_2 and C_2-Cl_3 (175.5 - 175.7 pm).

The geometrical parameters derived from the positions of disordered atoms of **3z** were excluded from consideration.

Table 1. Observed Interatomic Distances (pm) in Chlorinated Bicyclo[1.1.1]pentane-1,3-dicarboxylic Acids and Methyl Esters.

	1	**2x**	**3z**[a]	**4x**	**9a**	**9x**	**10z**
	(X_1 = Cl, X_2 - X_6 = R = H)	(X_1 = X_2 = Cl, X_3 - X_6 = R = H)	(X_1 = X_2 = X_4 = Cl, X_3 = X_5 = X_6 = R = H)	(X_1 - X_4 = Cl, X_5 = X_6 = R = H)	(X_1 = X_3 = Cl, X_2 = X_4 - X_6 = H, R = CH_3)	(X_1 = X_2 = Cl, X_3 - X_6 = H, R = CH_3)	(X_1 = X_2 = X_4 = Cl, X_3 = X_5 = X_6 = H, R = CH_3)
C_1-C_2	155.9	154.2	147.0	155.8	154.5	155.5	155.7
C_1-C_4	155.8	156.0	160.2	155.9	155.4	155.9	154.6
C_1-C_5	155.3	156.7	162.0	157.4	156.6	155.8	155.9
C_3-C_2	154.9	155.3	146.6	156.0	155.0	155.4	155.4
C_3-C_4	154.6	156.5	159.4	155.4	156.1	155.7	156.1
C_3-C_5	155.6	155.1	160.9	158.0	155.3	156.6	156.3
C_1-C_6	149.1	149.3	149.6	149.6	149.2	149.6	150.1
C_3-C_7	149.3	149.3	149.6	149.3	149.2	149.5	150.1
C_6=O_1	122.7	121.7	121.2	124.0	120.3	119.8	119.6
C_6-O_2R	130.3	130.9	129.5	125.7	132.4	132.6	131.7
C_7=O_3	122.4	124.5	121.2	124.2	120.5	119.5	120.0
C_7-O_4R	129.3	127.4	129.5	126.0	132.9	132.0	132.2
C_2-X_1	176.4	176.6	178.4	177.8	178.1	177.2	176.6
C_2-X_2	-[b]	177.9	178.1	175.5	-[b]	177.9	177.2
C_4-X_3	-[b]	-[b]	-[b]	175.7	178.3	-[b]	-[b]
C_4-X_4	-[b]	-[b]	159.4[c]	178.2	-[b]	-[b]	176.6
C_5-X_5	-[b]	-[b]	-[b]	-[b]	-[b]	-[b]	-[b]
C_5-X_6	-[b]	-[b]	-[b]	-[b]	-[b]	-[b]	-[b]
$C_1 \bullet\bullet\bullet C_3$	187.1	188.2	189.0	190.3	189.2	188.9	189.5
$C_2 \bullet\bullet\bullet C_4$	211.9	215.2	212.4	219.0	213.3	215.2	210.7
$C_2 \bullet\bullet\bullet C_5$	218.1	214.4	213.4	212.9	217.2	213.9	213.8
$C_4 \bullet\bullet\bullet C_5$	214.4	214.6	218.2	212.7	210.6	214.9	217.1

[a] Interatomic distances are inaccurate due to crystal disorder. [b] The C-H distance on the BCP cage was set at 100.0 pm. [c] The bond appears to be anomalously short due to high crystal disorder.

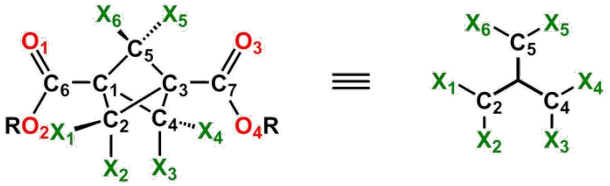

Figure 2. Labels for interatomic distances used in Table 2.

Computed Geometries of Bridge Chlorinated Bicyclo[1.1.1]pentanes. Geometries of all possible bridge chlorinated carboxylic acids were calculated with density functional theory (DFT) in the gas phase, and selected interatomic distances are collected in Table S2 (Supporting Information). Known compounds are highlighted in gray.

The computed interatomic distances reproduce the experimental trends. Substitution of hydrogen atoms on methylene bridges causes an increase of the interbridgehead distance from 186.8 pm in **0** to 193.3 pm in **6**; for each additional chlorine atom in the cage the interbridgehead distance increases by ~1.1 pm. This trend is observed both in measured and calculated C-Cl bond lengths in **4x**. The C-Cl bonds in **6** are longer than average.

Computed Strain Energy. The strain increase in compounds **1** - **6** relative to **0** was calculated using the hypothetical reaction shown in Scheme 5, where *n* and *m* are the numbers of C atoms carrying one and two chlorine atoms, respectively.

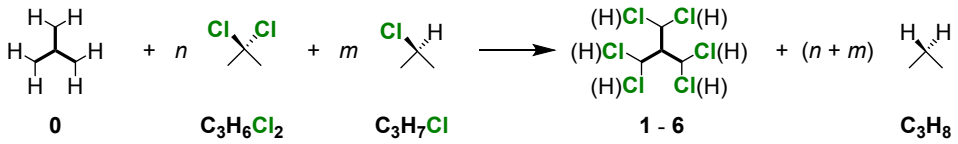

Scheme 5. Hyperhomodesmotic reactions for the estimation of strain energies.

For example, the strain for diacid **5**, which has five chlorine atoms, was calculated using Equation 1.

$$\mathbf{0} + 2 \times \mathbf{C_3H_6Cl_2} + \mathbf{C_3H_7Cl} \rightarrow \mathbf{5} + 3 \times \mathbf{C_3H_8} \quad (1)$$

The process conserves both the number of carbon-carbon bond types and the number of each type of carbon atoms (sp^3, sp^2, sp) and satisfies the criteria for hyperhomodesmotic reactions.[35] Calculated relative strain energies for all possible chlorinated derivatives of **0** are presented in Table 2.

Table 2. Calculated Relative Strain Energies (kcal/mol) in Chlorinated Bicyclo[1.1.1]pentane-1,3-dicarboxylic Acids.[a]

Cmpd.	Strain energy (kcalmol$^{[1]}$)	Cmpd.	Strain energy (kcalmol$^{[1]}$)
0	0	**3y**	17.63
1	2.46	**3z**	12.14
2a	6.25	**4a**	24.90
2x	6.56	**4x**	26.32
2y	7.22	**4y**	25.13
2z	11.11	**4z**	30.69

3a	12.84	**5**	43.68
3x	16.43	**6**	74.15

[a] Known compounds are highlighted in gray.

The calculated strain does not grow evenly as hydrogen atoms are gradually substituted by chlorines. Combinations of substituents that place H and Cl, and even more so, Cl and Cl, into syn contact cause additional strain. Up to the tetrachlorinated diacids, the steric crowding that results from these syn contacts can be partially alleviated by distortion of the threefold symmetry about the bridgehead-bridgehead axis and strain energies are very approximately additive. They can be estimated to within a few kcal/mol by assigning about 3 kcal/mol of strain to each syn H,Cl contact and about 15 kcal/mol of strain to each syn Cl,Cl contact. In penta- and hexachlorinated diacids, relief of strain by this type of angular distortion is no longer available, and the strain introduced by the two or three Cl,Cl syn contacts is disproportionately high, 43.68 kcal/mol in **5** and 74.15 kcal/mol in **6**.

The effect of syn contacts can be illustrated by examples. Three of the dichlorinated diacids, **2a**, **2x**, and **2y**, have two syn H,Cl contacts each, and have similar relative strain energies (6.25 - 7.22 kcal/mol), but the fourth one **2z**, with one syn Cl,Cl contact, has almost twice as much strain (11.11 kcal/mol). Similarly, two of the trichlorinated diacids (**3a** and **3z**) have three syn H,Cl contacts but no Cl,Cl contacts and are significantly less strained (12.14 and 12.84 kcal/mol) than the other two structures (**3x** and **3y**) that have one H,Cl and one Cl,Cl syn contact, with strain energies 16.43 and 17.63 kcal/mol, respectively. Diacid **4z**, with two Cl,Cl syn contacts, is more strained (30.69 kcal/mol) than the isomers **4a**, **4x**, and **4y**, which have only one Cl,Cl and two H,Cl syn contacts, and whose strain lies between 24.90 and 26.32 kcal/mol.

Due to the hyperhomodesmotic scheme used, the relative strain energies do not correspond to relative energies (i.e., stabilities). The most important difference is that geminal dichlorides are less stable than their vicinal isomers (Table S3 in Supporting Information). For example, the strain energies of **2a** and **2y** are virtually identical, but the geminal **2x** is about 5 kcal/mol less stable than the vicinal **2a**.

Computed Radical Abstraction Paths. In these computations, zero-point vibration energies were included.

(i) Chlorination. Halogenation of **2x** starts with hydrogen abstraction performed by a chlorine radical approaching the methylene bridge either from the syn or anti side relative to the CCl_2 bridge (Scheme 6). The CHCl units are nearly linear in both cases. The transition state for the anti approach is –0.7 kcal/mol lower in energy than that for the syn approach and results in the more stable radical $\mathbf{2x^{\bullet}_{anti}}$ (–4.3 vs. –4.9 kcal/mol for $\mathbf{2x^{\bullet}_{syn}}$). The interconversion of $\mathbf{2x^{\bullet}_{syn}}$ to $\mathbf{2x^{\bullet}_{anti}}$ involves a barrier of –0.8 kcal/mol. Their further barrierless chlorination can lead to **3y** and **3z**, respectively.

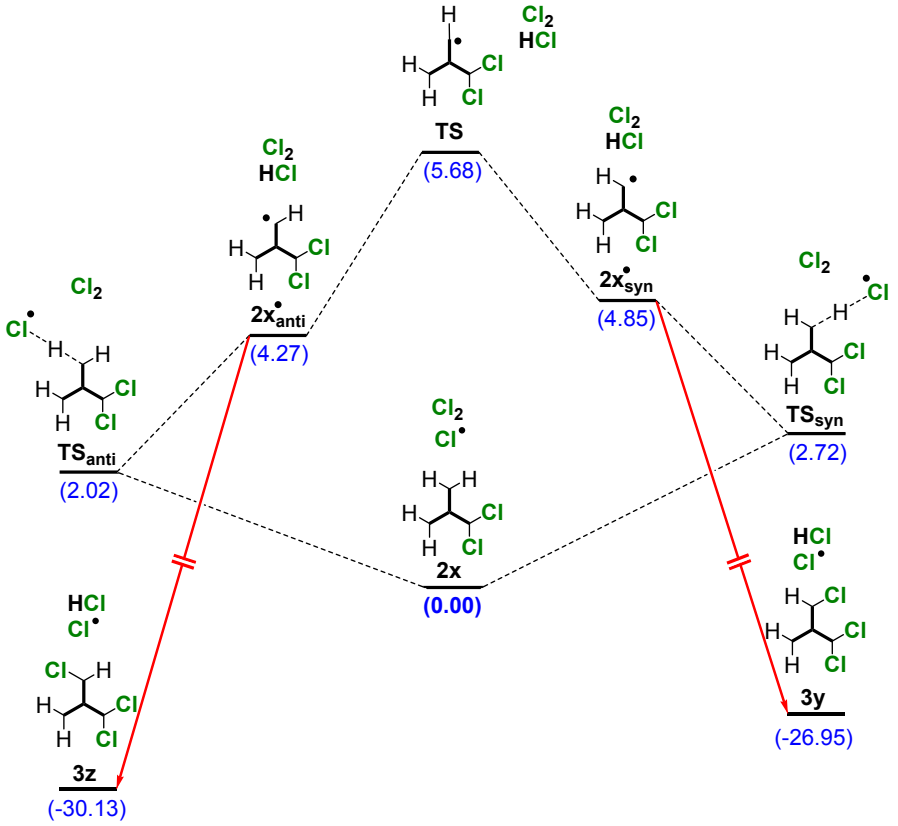

Scheme 6. Formation of **3y** and **3z** from **2x**.

Further chlorination of **3y** and **3z** occurs in similar manner (Scheme 7). The CHCl units in both transition states are linear again. Surprisingly, the barriers are different. The formation of **3z**• proceeds with a barrier of −3.3 kcal/mol, while the **3y**• is formed without any barrier. The energies of **3y**• and **3z**• differ by −1 kcal/mol in favor of the latter, but their interconversion involves a relatively high barrier of −5.8 kcal/mol.

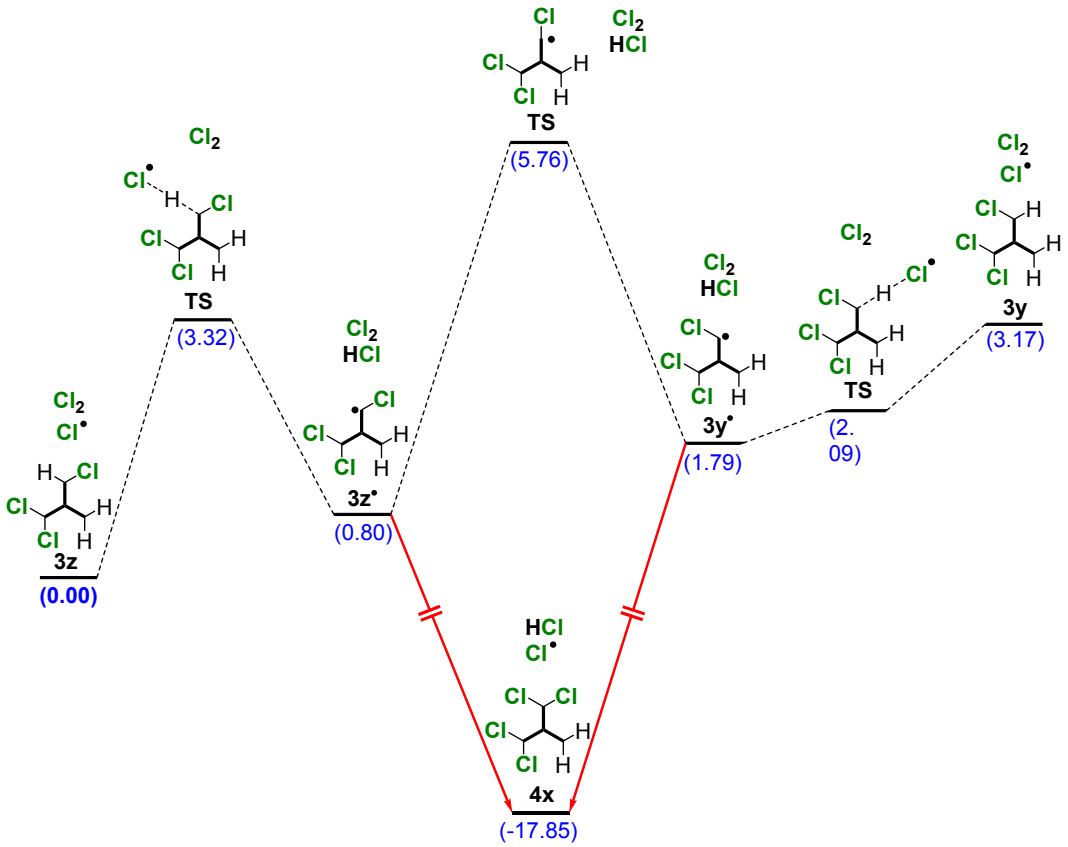

Scheme 7. Possible formation of **4x** from **3z** and **3y**.

(ii) Hydrodechlorination. Scheme 8 presents the energies of the pyramidalized radicals potentially involved in the hydrodechlorination of **3z** and the activation energies of their interconversion. The stereoisomer **2a**• is ~1.5 kcal/mol more stable than **2y**•. In the transition structures for chlorine atom abstraction the CClSi unit is close to linear, and the activation energies for the formation of **2a**• and **2y**• are very close to zero. The conversion of **2a**• into **2y**• involves a barrier of ~8 kcal/mol. The CHSi units in the transition structures for hydrogen transfer are also nearly linear and both activation energies are again negligible.

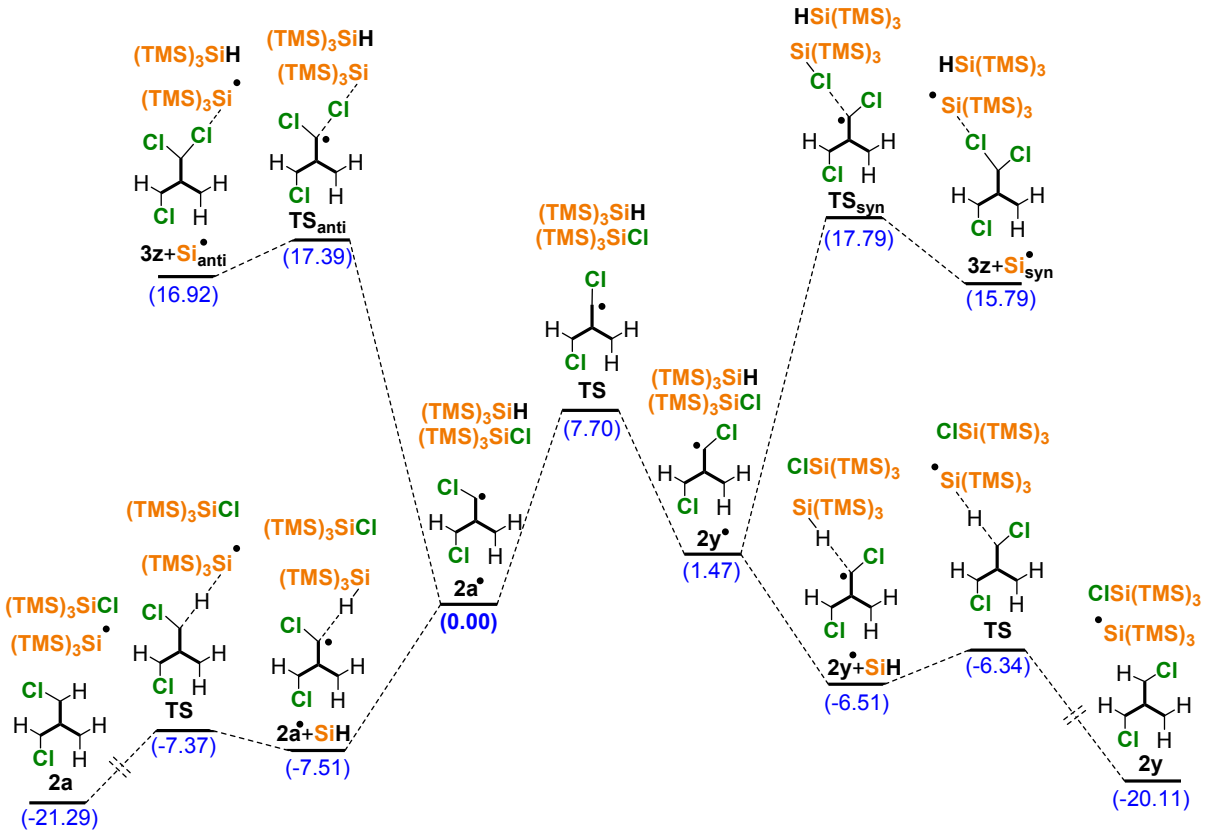

Scheme 8. Dehydrochlorination of dimethyl ester of **3z**.

Acidity Constants (pK_a). The pK_a values were measured in water solutions by capillary electrophoresis (CE). The mixed acidity constants, pK_a^{mix}, related to the activity of hydroxonium cations at 25 mM ionic strength, and the ionic mobilities μ_{1-} and μ_{2-} of the mono- and divalent anions of the diacids **0**, **1**, **2a**, **2x**, **3y**, and **4y**, were determined by nonlinear regression analysis of the pH dependence of their effective mobilities measured in a series of background electrolytes within a pH range of 0.92 - 5.51 at constant ionic strength (25 mM) and temperature (25 °C). These pK_a^{mix} values were converted to the thermodynamic acidity constants pK_a^{th} using the Debye-Hückel theory.[36] The mixed and thermodynamic pK_a values and ionic mobilities are summarized in Table 3.

Table 3. Acidity Constants pK_a of 0, 1, 2a, 2x, 3z, and 4x at 25 EC.[a]

Cmpd.	p$K_{a,1}^{th}$	p$K_{a,2}^{th}$	p$K_{a,1}^{mix}$	p$K_{a,2}^{mix}$	μ_{1-} (10^{-9}m^{2}V^{-1}s^{-1})	μ_{2-} (10^{-9}m^{2}V^{-1}s^{-1})
0[b]	**2.78 ± 0.08**	**4.14 ± 0.10**	2.71 ± 0.08	3.94 ± 0.10	-19.0 ± 0.0	-37.9 ± 0.9
1	**2.24 ± 0.07**	**3.49 ± 0.09**	2.17 ± 0.07	3.28 ± 0.09	-19.0 ± 0.0	-38.2 ± 0.7
2a	**1.82 ± 0.05**	**2.90 ± 0.07**	1.75 ± 0.05	2.69 ± 0.07	-19.0 ± 0.0	-38.0 ± 0.5
2x	**1.86 ± 0.05**	**3.05 ± 0.07**	1.79 ± 0.05	2.84 ± 0.07	-19.0 ± 0.0	-37.8 ± 0.5
3z	**1.43 ± 0.03**	**2.57 ± 0.04**	1.36 ± 0.03	2.36 ± 0.04	-19.0 ± 0.0	-37.1 ± 0.3
4x	**1.07 ± 0.03**	**2.31 ± 0.03**	1.00 ± 0.03	2.10 ± 0.03	-19.0 ± 0.0	-37.5 ± 0.2

[a] pK_a^{th}: thermodynamic acid dissociation constant (at zero ionic strength), pK_a^{mix}: mixed acid dissociation constant at ionic strength 25 mM, μ_{1-} and μ_{2-}: ionic mobilities of the univalent and divalent anionic forms of the analyzed acids. [b] Previously published values obtained by potentiometric titration: $pK_{a,1} = 3.22 \pm 0.02$, $pK_{a,2} = 4.26 \pm 0.03$.[32]

In order to estimate the acidity of **5** and **6**, the B3LYP-D3/6-311+G(d,p) results obtained using the cluster-continuum model (two explicit molecules of water plus SMD) were compared with measured pK_a values of **0**, **1**, **2a**, **2x**, **3y**, and **4y** (Table 3). A good linear correlation (R^2 = 0.91, Figure S4 in Supporting Information) was found between the calculated reaction energies and the measured acidities, producing a mean unsigned error of 0.22 for predicted pK_a values, shown in Table 4. The errors of the predicted values appear to be uniformly distributed (plot of residuals in Supporting Information), suggesting that the predictions for **5** and **6** should be within the same error margins as **0**, **1**, **2a**, **2x**, **3y**, and **4y**.

Table 4. Predicted pK_a Values for Compounds 0, 1, 2a, 2x, 3y, 4y, 5, and 6 with Absolute Deviations from Measured Values.

Cmpd.	$pK_{a,1}$	Error	$pK_{a,2}$	Error
0	3.16	0.38	4.07	0.07
1	2.66	0.42	3.27	0.22
2a	1.90	0.08	2.73	0.17
2x	2.17	0.31	2.84	0.21
3y	1.59	0.16	2.35	0.22
4y	0.97	0.1	1.97	0.34
5	0.64	-	1.27	-
6	0.28	-	0.77	-

NMR Spectroscopy. Results obtained from ^{1}H, ^{13}C, ^{13}C APT (Attached Proton Test), HSQC (Heteronuclear Single Quantum Coherence) and HMBC (Heteronuclear Multiple Bond Correlation) spectra of **0**, **1**, **2a**, **2x**, **3y**, and **4y** are collected in Figure 3. The proton NMR spectrum of **2x** exhibits a complex AA'BB' pattern and the geminal and ^4J coupling constants were therefore extracted from ^{13}C satellites. To confirm the assignment of the signals and couplings further, we compared the experimental data with those calculated by DFT. The agreement is very good (Figures S5 and S6 in Supporting Information).

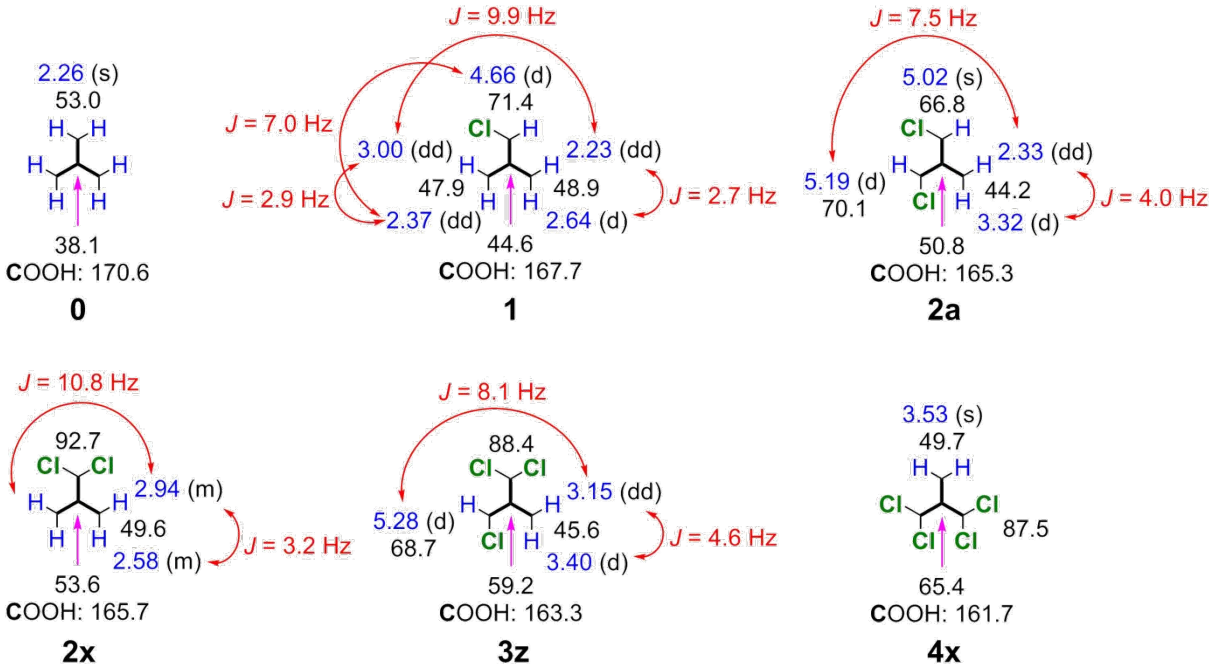

Figure 3. Proton (blue) and carbon (black) NMR chemical shifts for **0**, **1**, **2a**, **2x**, **3z**, and **4x** measured in acetone-d_6 at 25 °C. Proton-proton coupling constants are shown in red.

DISCUSSION

Chlorination of Methylene Bridges. Unlike fluorination, the chlorination of bicyclo[1.1.1]pentane1,3-dicarboxylates in the form of their dichlorides is fairly selective and favors the formation of certain isomers, while others are inaccessible. The abstraction of the first hydrogen atom from one of the CH_2 bridges is relatively difficult, but the presence of the first chlorine atom on a CHCl bridge dramatically increases the rate of abstraction of the second hydrogen (Scheme 1A). This is attributable to the radical stabilizing effect of the first chlorine.[27] As a result, the yield of the monochlorinated product is poor and the only directly dichlorinated diacid that results in useful yield after methanolysis and hydrolysis is the geminal **2x**. The isomers **2a**, **2y**, and **2z** are not accessible by direct chlorination.

Subsequent chlorination of the dichloride of the geminally dichlorinated diacid **2x** (Scheme 1B) starts with the abstraction of a hydrogen atom from one of the remaining two CH_2 bridges. The resulting bridge radical is surrounded by a bulky CCl_2 bridge on one side and a much smaller CH_2 bridge on the other. It abstracts a chlorine atom from Cl_2 more readily at the face that is adjacent to the CH_2 and not the CCl_2 bridge, probably not only because this face is less hindered, but also because at the transition state there is a sigma-conjugated W-shaped path to one of the geminal chlorine atoms.[37] Attack at this face ultimately produces the trichlorinated diacid **3z** to the exclusion of the isomer **3y**, which would require an attack at the face adjacent to the CCl_2 bridge (Scheme 6).

The dichloride of the trichlorinated diacid **3z** has two bridges that could be further chlorinated, CHCl and CH_2. Activation by the already present chlorine atom overcomes the effect of steric hindrance and abstraction of the next hydrogen atom occurs exclusively on the more hindered CHCl bridge (Scheme 7). The need to overcome steric problems undoubtedly is the reason why much harsher reaction conditions are required. The doubly geminal **4x** is thus the only tetrachlorinated diacid that results after workup of the reaction mixture (Scheme 1C), in spite of its 26.32 kcal/mol calculated strain associated with the steric repulsion in its syn Cl,Cl contact. The strain is comparable with that in the previously published penta- and

hexafluorinated bicyclo[1.1.1]pentane-1,3-dicarboxylic acid analogs (21.8 and 32.9 kcal/mol, respectively).30 The slightly less strained tetrachlorinated diacids that would result from substitution of hydrogen atoms on the CH_2 bridge (**4y**, 25.13 kcal/mol, and **4a**, 24.90 kcal/mol) are not formed.

The highly strained **4x** seems to be surprisingly stable and even extended chlorination of its dichloride did not cause any degradation of its bicyclic cage. A thorough examination of the reaction mixture by ^{1}H NMR and MS revealed a trace of a compound that could be assigned as a double methyl ester of a pentachlorinated diacid, but it was not isolated and its structure remains unproven. Calculations suggest that the introduction of a fifth chlorine atom to the bicyclic cage will increase the relative strain energy by an additional ~20 kcal/mol, to 43.68 kcal/mol in **5**. Substitution of the last hydrogen atom in **5** by chlorine should lead to perchlorinated **6**, whose enormous calculated strain (74.15 kcal/mol) would exceed the strain of the bicyclic cage itself (68 kcal/mol[38]), and would be only slightly lower than the standard strength of the C-Cl (81 - 84 kcal/mol) and C-C (83 - 85 kcal/mol) bonds.[39]

Reduction of Chlorinated Cages. Reduction of the polychlorinated diesters with TMS_3SiH opens a synthetic path to isomers that are not accessible by direct chlorination. We have revised the previously published related procedures20,27 and were able to significantly increase isolated yields by careful control of reaction conditions. Monitoring of the progress of the reaction allowed us to draw the following conclusions: (i) the reduction of **9x** and **10z** to **8** and **9a**, respectively, is a clean and quantitative process, but imperfect product isolation reduces the yields slightly, (ii) reactions performed in benzene-d_6 do not lead to incorporation of deuterium into the final products.

The reduction of **9x** that affords monochlorinated **8** in high isolated yield was published before27 and does not require any additional comment. In contrast, an explanation is needed for the perfect specificity with which the reduction of the trichlorinated double methyl ester **10z** of the diacid **3z** leads solely to the dichlorinated double ester **9a** derived from the diacid **2a** and none of the also expected dichlorinated double ester derived from the diacid **2y**, which is only 1 kcal/mol more strained (7.22 kcal/mol vs. 6.25 kcal/mol, Table 2). Similar trends were noticed previously in the fluorinated analogues.31

There is little doubt that the reaction of **10z** is initiated by the abstraction of one of the geminal chlorine atoms by the tris(trimethylsilyl)silyl radical to yield a chlorine-stabilized bridge radical, and the question that needs to be answered is why this radical abstracts a hydrogen from tris(trimethylsilyl)silane at the face adjacent to the CH_2 bridge and not the face adjacent to the CHCl bridge (Scheme 8). The calculations do not provide a reliable argument for differentiating the rates of formation of **2a**$^\bullet$ and **2y**$^\bullet$, but they provide their relative stabilities. If their interconversion is fast enough to establish an equilibrium, the ratio of their concentrations is of the order of 8:1 at 80 EC, and if the rates of hydrogen abstraction by these two radicals are similar, the expected ratio of **2a** and **2y** will also be 8:1. Then, the actually observed product **2a** is indeed predicted to be dominant, but not as exclusively as is observed.

It is interesting to ask why **2a**$^\bullet$ is more stable than **2y**$^\bullet$. Steric conditions appear to be similar at both faces, but stereoelectronic conditions are different. Only abstraction at the CH_2 bridge face offers a W-shaped sigma-conjugation path for donation of electron density from the electropositive Si atom of the silane to the electronegative Cl atom on the CHCl bridge, stabilizing the hydrogen abstraction transition state, while abstraction at the CHCl bridge offers a destabilizing W-shaped interaction path between two C-Cl bonds.37

An attempt to reduce **11x** under the same conditions led to a complete destruction of the bicyclic cage and only traces of **10z** were detected in the crude reaction mixture (Scheme

9). The reaction was fast and the starting **11x** was completely consumed in less than 30 min, although the same kind of reduction performed on **9x** or **10z** required more than 10 hours for completion. It is likely that strain relief promotes the abstraction of chlorine atom.

The radical that results from the abstraction of a chlorine atom from **11x** by a silyl radical has nominally the same cage as that produced by the abstraction of a hydrogen atom from **3z** by a chlorine atom. Yet, the final products of the two reactions are very different. The former leads to a breakdown of the bicyclic cage, whereas the latter produces an almost quantitative yield of **4x**. Two factors come to mind as a possible explanation, and both could play a role. (i) The difference in the reaction products could be due to the difference of the concentrations of the reaction partners in the two cases. The conversion of **3z** to **4z** occurs in liquid chlorine, undoubtedly giving the intermediate radical very little time to rearrange and lose its cage structure, whereas the abstraction of a Cl atom from **11x** occurs in a relatively dilute solution in benzene, with a much longer time during which this rearrangement can occur. (ii) The radicals formed in the two abstraction reactions could only nominally have identical cages and in reality could differ in the sense of pyramidalization. If their interconversion is slow on the reaction time scale, each can give different products. This is illustrated in Schemes 6 and 8, assuming that the abstraction of hydrogen and chlorine occurs with retention of configuration. This issue deserves closer attention but lies outside the scope of the present paper.

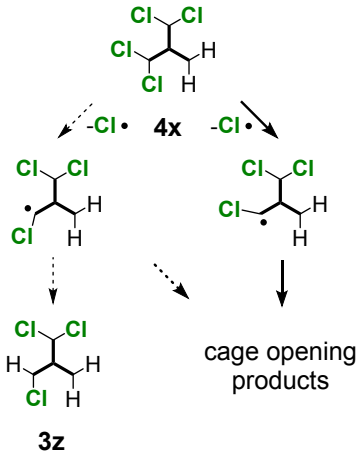

Scheme 9. Attempted hydrodechlorination of **4x**.

Structure of the Chlorinated Cages. The changes in structural parameters that describe the bicyclic cage as the number of chlorine substituents increases are relatively minor and can be understood simply. Thus, Bent's rules account for the increase in the CCC valence angle at bridge carbons with increasing number of chlorine substituents, which causes an increase in the inter-bridgehead distance. The calculated increase in the C-Cl bond lengths in **6** can be understood as a result of non-bonded Cl - Cl repulsions.

Saponification of Methyl Esters. Basic hydrolysis of **8**, **9a**, **9x**, **10z**, and **11x** performed under homogenous reaction conditions (LiOH in a THF/water mixture) proceeds as expected and yields salts of the acids **1**, **2a**, **2x**, **3z**, and **4x** in nearly quantitative yields. In contrast, heterogenous hydrolysis of **9x** with aqueous NaOH at a slightly elevated temperature of 50 °C afforded after workup in addition to **2x** also an unexpected cyclobutene derivative **12** that was characterized as the methyl ester **13** (Scheme 4). We did not examine this transformation in detail, but propose a possible mechanism for the observed outcome.

The cage opening starts with an unprecedented attack by hydroxide anion at one of the methylene bridges in **9x**, which leads to C-C bond breaking and stabilization of the negative charge by conjugation with the COOR group. Subsequent elimination of a chloride anion produces the cyclobutene ring.

Acidity Constants in Water. The acidity of parent **0** ($pK_{a,1}$ = 2.78 ± 0.08, $pK_{a,2}$ = 4.14 ± 0.10) determined by capillary electrophoresis is higher than the previously published32 values obtained by potentiometric titration ($pK_{a,1}$ = 3.22 ± 0.02, $pK_{a,2}$ = 4.26 ± 0.03). Acidity is increased by chlorine substitution on the methylene bridges in an almost additive manner: $pK_{a,1}$ drops by about half a pH unit upon each Cl for H replacement, and $pK_{a,2}$ drops slightly more. This can be compared with the effect of a single chlorine atom in the β position of propionic acid, which lowers the pK_a value by 0.77 pK units.[40] The four chlorine atoms in **4x** increase each of the acidities by 1.7 - 1.8 pH units, and the acidities of the isomeric dichlorinated acids **2a** and **2x** are nearly identical (Table 3).

The calculated pK_a values of **0**, **1**, **2a**, **2x**, **3z**, and **4x** correlate reasonably well with the measured numbers and this allows us to predict the acidities of **5** and **6**. The introduction of the fifth chlorine atom in **5** lowers both pK_a values, to 0.64 and 1.27. The hexachlorinated diacid **6** follows the same trend to the exceptionally low computed values of $pK_{a,1}$ = 0.28 and $pK_{a,2}$ = 0.77. This diacid should be even more acidic than the corresponding perfluorinated analogue ($pK_{a,1}$ = 0.73 and $pK_{a,2}$ = 1.34).[32]

Nuclear Magnetic Resonance Spectroscopy. Comparison of ^{13}C NMR chemical shifts of chlorinated diacids **1**, **2a**, **2x**, **3z**, and **4x** with the parent diacid **0** allow us to draw the following conclusions: (i) resonances of CH_2 bridges in **1**, **2a**, **2x**, **3z**, and **4x** usually appear at 44.2 - 49.7 ppm, slightly above that in **0** (53.0 ppm). (ii) Substitution of one hydrogen atom by chlorine on a CH_2 bridge shifts its carbon resonance ~16 ppm downfield and signals of CHCl units are found at 66.8 - 71.4 ppm. (iii) Replacement of the second hydrogen shifts the signal by an additional ~21 ppm downfield and signals of CCl_2 units appear at 87.5 - 92.7 ppm. (iv) Resonances of the bridgehead carbons are sensitive to chlorine substitution at the bridges: 38.1 ppm in **0** and 65.4 ppm in **4x**. Each chlorine atom on a bridge shifts the resonance of the bridgehead carbon atoms ~7 ppm downfield. (v) An opposite but weaker trend is observed for chemical shifts of carboxylic carbon atoms: each chlorine atom on a methylene bridge shifts them upfield by ~2.2 ppm, from 170.6 ppm in **0** to 161.7 ppm in **4x**.

SUMMARY

Three new bridge-chlorinated bicyclo[1.1.1]pentane derivatives were synthesized and their preferential formation was rationalized. The remarkable stereoselectivity in both the introduction and the removal of chlorine atoms can be understood in terms of steric and stereoelectronic effects (sigma conjugation). All five known bridge-chlorinated cages were analyzed by X-ray diffraction and the results showed that each chlorine atom attached to the cage increases the inter-bridgehead separation. Acidities of the dicarboxylic acids were determined both by capillary electrophoresis and computationally and the results were in good agreement. Substitution of each hydrogen atom by chlorine decreases both pK_a values.

EXPERIMENTAL SECTION

Materials. All reactions were carried out under argon atmosphere with dry solvents freshly distilled under anhydrous conditions, unless otherwise noted. Standard Schlenk and vacuum line techniques were employed for all manipulations of air- or moisture-sensitive compounds. Yields refer to isolated, chromatographically and spectroscopically homogenous materials, unless otherwise stated.

Bicyclo[1.1.1]pentane-1,3-dicarboxylic acid (**0**) was synthesized according to a published procedure.34 THF and ether were dried over sodium with benzophenone and distilled under argon prior to use. Benzene-d_6 was dried over sodium and distilled under argon prior to use. Carbon tetrachloride was dried over CaH_2 and distilled under argon prior to use. All other reagents were used as supplied unless otherwise stated.

Procedures. Analytical thin-layer chromatography (TLC) was performed using precoated TLC aluminum sheets (Silica gel 60 F_{254}). TLC spots were visualized using either UV light (254 nm) or a 5% solution of phosphomolybdic acid in ethanol, and heat (400 °C) as a developing agent. Flash chromatography was performed using silica gel (high purity grade, pore size 60 Å, 70 - 230 mesh). Melting points are reported uncorrected. Infrared spectra (IR) were recorded in KBr pellets. Chemical shifts in ^{1}H and ^{13}C NMR spectra are reported in ppm on the δ scale relative to $CHCl_3$ (δ = 7.26 ppm for ^{1}H NMR and δ = 77.0 ppm for ^{13}C NMR) and acetone-d_6 (δ = 2.05 ppm for ^{1}H NMR and δ = 29.8 ppm for ^{13}C NMR) as internal references. Splitting patterns are assigned as s = singlet, d = doublet, t = triplet, m = multiplet, br = broad signal.

High-resolution mass spectra (HRMS) using atmospheric-pressure chemical ionization (APCI) and electrospray ionization (ESI) were obtained on a mass analyzer combining linear ion trap and the Orbitrap, and those using chemical ionization (CI) mode were taken on a time-of-flight mass spectrometer.

X-ray Diffraction. Crystallographic data were collected on Bruker D8 VENTURE Kappa Duo PHOTON100 by IμS micro-focus sealed tube either with MoKα radiation (λ = 0.71073 Å) **1**, **2x**, **4x**, and **9x** or CuKα radiation (λ = 1.54178 Å) **2a**, **9a**, and **10z**. The measurements were performed at 150 K, except for **4x**, which was measured at 200 K, because of a phase transition at a lower temperature. The structures were solved by direct methods (XT)[41] and refined by full matrix least squares based on F^2 (SHELXL2014).[42] The hydrogen atoms on carbon atoms were fixed into idealized positions (riding model) and assigned temperature factors of either $H_{iso}(H) = 1.2\ U_{eq}$(pivot atom) or $H_{iso}(H) = 1.5\ U_{eq}$ (pivot atom) for methyl moiety. The hydroxyl hydrogens were found on difference electron density map and refined as riding on the corresponding oxygen atom.

The molecules of carboxylic acids in the study are prone to disorder in their crystal structures, mostly by rotation or mirroring of the bicyclic cage. The ruling contacts in their crystals assembly are doubled short hydrogen bonds C=O•••H-O-C of carboxylic moieties forming infinite chains.

In **1** three equatorial carbon atoms of bicyclo[1.1.1]pentane are disordered over two locations, whereas the chlorine atom keeps its place.

The diacid **3z** is disordered in a more complicated manner. The equatorial carbon atoms are again disordered in two positions, each along operation of inversion of the space group. Three chlorine atoms are distributed in four positions; such distribution is expected to have two positions fully occupied and two with one-half occupation factor. However this is not the case, the positions are overlapped twice so the maximum occupation factor is 0.82769 and the minimum factor is 0.67231. They were refined with restriction to give the proper formula.

The most complicated disorder is found in **2a**. Two symmetrically independent molecules form two infinite chains. The first chain is ordered while the second one is totally disordered. All attempts to resolve this disorder led to high R-factors and large maxima on difference Fourier maps. Therefore the refinements were focused on the ordered part, allowing the disordered molecules to acquire any geometry and displacement factors.

Calculations. Prior to DFT optimizations, MM2-level systematic conformational scans were performed by varying the torsional angles between the two carboxylic groups and the central carbon atoms in increments of 5°, with 5 optimization steps performed in each scan increment.

The minima obtained in the previous step were then optimized using the B3LYP functional, which has been extensively used to produce good estimates of strain energies.[43,44,45,46] A 6-311+G(d,p) triple-split basis set was used, and diffuse functions were included to describe both the effect of the chlorine atoms and the negatively charged conjugate bases more accurately. Also, empirical corrections for long-range interactions were done using Grimme´s dispersion with Becke-Johnson damping (B3BJ).[47]

To estimate pK_a values, optimizations of **0**, **1**, **2a**, **2x**, **3z**, **4x**, **5**, and **6** were repeated using the B3LYP-D3BJ/6-311+G(d,p) method in conjunction with Truhlar´s SMD implicit solvent model,[48] followed by frequency calculations. In order to improve the description of solvation, two explicit water molecules were added to all structures.[49,50] These water molecules were always placed the same manner, each forming a single hydrogen bond with a different carboxylic group. The number of analyzed conformers grew substantially: starting from each gas-phase geometry of a neutral compound, up to four different conformers for monoanions and another four for dianions were constructed. However, the resulting relative energies of different conformers were generally very similar (within 0.4 kcal/mol). The same method was used for the radical involving paths with the appropriate solvents (CCl_4 and benzene).

For all above mentioned calculations, only the lowest energy structure of each compound was used. These calculations were done using Gaussian 09.[51]

NMR chemical shifts and coupling constants were calculated using B3LYP functional, 6-31G(d,p) basis set and polarizable continuum model used for implicit acetone solvation.[52,53] The Gaussian 16 program package was used for the NMR calculations.[54]

Measurements of pK_a. Capillary electrophoresis (CE) experiments were performed on a CE 7100 analyzer (Agilent, Waldbronn, Germany) equipped with UV-vis spectrophotometric diode array detector set at 200 nm and bare fused silica capillary with outer polyimide coating: id/od 50/375 μm, total/effective (to the detector) length 480/395 mm, Polymicro Technologies, Phoenix, AZ, USA.

Synthesis. Hydrolysis of Methyl Esters (GP1). Dimethyl esters **8**, **9a**, **9x**, **10z**, and **11x** (1 equiv.) were dissolved in wet THF (6 mL) and $LiOH.H_2O$ (10 equiv.) followed by water (4 mL) was added to the reaction mixture. The slightly yellowish solution was stirred for 60 min at room temperature. Subsequently, THF was removed under reduced pressure and the aqueous phase was acidified with concentrated aqueous HCl to pH ~1. White dense solid precipitated in most cases. The aqueous phase was extracted with ether (3 × 25 mL) and the colorless organic phase was dried over $MgSO_4$. The solvent was removed under reduced pressure and the slightly yellowish solid residue was triturated with CH_2Cl_2 (3 × 2 mL), hexane (3 × 2 mL), and finally thoroughly dried under reduced pressure (60 min, 600 mTorr). Diacids **1**, **2a**, **2x**, **3z**, and **4x** were obtained as white or slightly grayish crystalline solids.

2-Chlorobicyclo[1.1.1]pentane-1,3-dicarboxylic Acid (**1**) was prepared from **8** (90 mg, 0.412 mmol) and $LiOH.H_2O$ (173 mg, 4.120 mmol) in a mixture of THF (6 mL) and water (4 mL) according to **GP1**. Compound **1** was obtained as a grayish crystalline solid (68 mg, 0.357 mmol, 87%).

Mp > 243 °C (dec.). ^{1}H NMR (400 MHz, acetone-d_6): δ 2.23 (dd, J_1 = 2.7 Hz, J_2 = 9.9 Hz, 1H), 2.37 (dd, J_1 = 2.9 Hz, J_2 = 7.0 Hz, 1H), 2.64 (d, J = 2.7 Hz, 1H), 3.00 (dd, J_1 =

2.9 Hz, J_2 = 9.9 Hz, 1H), 4.66 (d, J = 7.0 Hz, 1H), 9.89 (br s, 2H). ^{13}C {^1H} NMR (100 MHz, acetone-d_6): δ 44.6, 47.9, 48.9, 71.4, 167.7. IR (KBr): 3029, 2987, 2919, 2612, 1706, 1502, 1428, 1339, 1300, 1221, 1089, 1059, 1014, 927, 811, 748, 599, 529, 472 cm^{-1}. MS, *m/z* (%): 189.0 (100, center of isotope cluster, M - H). HRMS (ESI-) *m/z*: [M - H]$^-$ Calcd for $C_7H_6ClO_4^-$ 188.9960; Found 188.9961. Anal. Calcd. for $C_7H_7ClO_4$: C, 44.12; H, 3.70. Found: C, 44.26; H, 3.75.

(*1RS, 2rs, 3SR, 4sr*)-2,4-Dichlorobicyclo[1.1.1]pentane-1,3-dicarboxylic Acid (**2a**) was prepared from **9a** (120 mg, 0.474 mmol) and LiOH.H_2O (199 mg, 4.740 mmol) in a mixture of THF (6 mL) and water (4 mL) according to **GP1**. Compound **2a** was obtained as a grayish crystalline solid (97 mg, 0.431 mmol, 91%).

Mp > 263 °C (dec.). ^1H NMR (400 MHz, acetone-d_6): δ 2.33 (dd, J_1 = 4.0 Hz, J_2 = 7.5 Hz, 1H), 3.32 (d, J = 4.0 Hz, 1H), 5.02 (s, 1H), 5.19 (d, J = 7.5 Hz, 1H), 9.84 (br s, 2H). ^{13}C {^1H} NMR (100 MHz, Acetone-d_6): δ 44.2, 50.8, 66.8, 70.1, 165.3. IR (KBr): 3022, 2907, 2625, 2583, 1710, 1528, 1478, 1430, 1347, 1303, 1217, 1144, 1111, 1077, 1060, 1005, 944, 883, 774, 755, 734, 714, 692, 550, 492, 476 cm^{-1}. MS, *m/z* (%): 223.0 (100, center of isotope cluster, M - H). HRMS (ESI-) *m/z*: [M - H]$^-$ Calcd for $C_7H_5Cl_2O_4^-$ 222.9570; Found 222.9572. Anal. Calcd. for $C_7H_6Cl_2O_4$: C, 37.36; H, 2.69. Found: C, 37.38; H, 2.67.

2,2-Dichlorobicyclo[1.1.1]pentane-1,3-dicarboxylic Acid (**2x**) was prepared from **9x** (200 mg, 0.790 mmol) and LiOH.H_2O (331 mg, 7.900 mmol) in a mixture of THF (6 mL) and water (4 mL) according to **GP1**. Compound **2x** was obtained as a white crystalline solid (172 mg, 0.764 mmol, 97%).

Mp > 255 °C (dec.). ^1H NMR (400 MHz, acetone-d_6): δ 2.58 (m, 2H), 2.94 (m, 2H), 9.65 (br s, 2H). ^{13}C {^1H} NMR (100 MHz, acetone-d_6): δ 49.6, 53.6, 92.7, 165.7. IR (KBr): 3362, 3038, 2921, 2731, 2611, 2515, 1706, 1502, 1430, 1340, 1304, 1216, 1148, 1132, 1068, 1027, 1015, 942, 883, 862, 829, 789, 756, 724, 704, 648, 577, 524, 485, 433 cm^{-1}. MS, *m/z* (%): 223.0 (100, center of isotope cluster, M - H). HRMS (ESI-) *m/z*: [M - H]$^-$ Calcd for $C_7H_5Cl_2O_4^-$ 222.9570; Found 222.9571. Anal. Calcd. for $C_7H_6Cl_2O_4$: C, 37.36; H, 2.69. Found: C, 37.23; H, 2.62.

(*1RS*, *3SR*, *4sr*)-2,2,4-Trichlorobicyclo[1.1.1]pentane-1,3-dicarboxylic Acid (**3z**) was prepared from **10z** (400 mg, 1.391 mmol) and LiOH.H_2O (584 mg, 13.910 mmol) in a mixture of THF (6 mL) and water (4 mL) according to **GP1**. Compound **3z** was obtained as a white crystalline solid (332 mg, 1.280 mmol, 92%).

Mp > 259 °C (dec.). ^1H NMR (400 MHz, acetone-d_6): δ 3.15 (dd, J_1 = 4.6 Hz, J_2 = 8.1 Hz, 1H), 3.40 (d, J = 4.6 Hz, 1H), 5.28 (d, J = 8.1 Hz, 1H). ^{13}C {^1H} NMR (100 MHz, Acetone-d_6): δ 45.6, 59.2, 68.7, 88.4, 163.3. IR (KBr): 3359, 3045, 2916, 2618, 2586, 2506, 1715, 1484, 1434, 1340, 1289, 1208, 1141, 1099, 1058, 1009, 922, 792, 748, 701, 602, 501, 442 cm^{-1}. MS, *m/z* (%): 256.9 (100, center of isotope cluster, M - H). HRMS (ESI-) *m/z*: [M - H]$^-$ Calcd for $C_7H_4Cl_3O_4^-$ 256.9181; Found 256.9180. Anal. Calcd. for $C_7H_5Cl_3O_4$: C, 32.40; H, 1.94. Found: C, 32.38; H, 1.92.

2,2,4,4-Tetrachlorobicyclo[1.1.1]pentane-1,3-dicarboxylic Acid (**4x**) was prepared from **11x** (200 mg, 0.621 mmol) and LiOH.H_2O (261 mg, 6.210 mmol) in a mixture of THF (6 mL) and water (4 mL) according to **GP1**. Compound **4x** was obtained as a white crystalline solid (160 mg, 0.544 mmol, 88%).

Mp > 195 °C (dec.). ^1H NMR (400 MHz, acetone-d_6): δ 3.53 (s, 2H). ^{13}C {^1H} NMR (100 MHz, acetone-d_6): δ 49.7, 65.4, 87.5, 161.7. IR (KBr): 3373, 3030, 2867, 2601, 2510, 1718, 1432, 1296, 1230, 1182, 1093, 1020, 973, 933, 844, 794, 753, 713, 665, 541, 509, 489, 418 cm^{-1}. MS, *m/z* (%): 292.9 (100, center of isotope cluster, M - H), 248.9 (52), 168.9 (63,

centre of isotope cluster). HRMS (ESI-) *m/z*: [M - H]$^-$ Calcd for $C_7H_3Cl_4O_4^-$ 290.8791; Found 290.8789. Anal. Calcd. for $C_7H_4Cl_4O_4$: C, 28.61; H, 1.37. Found: C, 28.63; H, 1.38.

Bicyclo[1.1.1]pentane-1,3-dicarbonyl Dichloride (**7**).34 A suspension of **0** (2.000 g, 12.809 mmol) in $SOCl_2$ (8.00 mL, 109.675 mmol) was refluxed 5 h at oil bath temperature of 100 °C. All solids slowly dissolved leaving a clear yellowish solution. Volatiles were distilled off at atmospheric pressure and the same temperature. Kugelrohr distillation of the yellow oily residue (130 °C, 600 mTorr) afforded **7** as colorless oil that immediately crystallized (2.398 g, 12.424 mmol, 97%).

Mp 58.3 - 60.0 °C (lit.[34] 55 - 57 °C). ^{1}H NMR (400 MHz, $CDCl_3$): δ 2.58 (s, 6H). ^{13}C {^{1}H} NMR (100 MHz, $CDCl_3$): δ 44.6, 54.8, 169.4.

Dimethyl 2-Chlorobicyclo[1.1.1]pentane-1,3-dicarboxylate (**8**). The published procedure20 was adapted as follows. To a solution of **9x** (115 mg, 0.454 mmol) in benzene-d_6 (10 mL) was added TMS_3SiH (169 µL, 0.545 mmol, 1.2 equiv.) and AIBN (19 mg, 0.114 mmol, 25mol%) at room temperature. The clear colorless reaction mixture was stirred 6 h at 80 °C and 14 h at 60 °C. Reaction progress was monitored by ^{1}H NMR (500 µL of the reaction mixture was injected into an NMR tube and directly measured; the analyzed sample was returned into the reaction mixture). Volatiles were removed under reduced pressure and column chromatography on silica gel (hexane/ethyl acetate - 6:1) afforded **8** as a clear colorless oil (93 mg, 0.425 mmol, 94%).

^{1}H NMR (400 MHz, $CDCl_3$): δ 2.17 (dd, J_1 = 2.9 Hz, J_2 = 9.9 Hz, 1H), 2.39 (dd, J_1 = 3.1 Hz, J_2 = 7.1 Hz, 1H), 2.58 (d, J = 2.9 Hz, 1H), 3.12 (dd, J_1 = 3.1 Hz, J_2 = 9.8 Hz, 1H), 3.73 (s, 6H), 4.52 (d, J = 7.1 Hz, 1H). ^{13}C {^{1}H} NMR (100 MHz, $CDCl_3$): δ 43.9, 48.1, 48.7, 52.2, 70.4, 166.8. IR (KBr): 3009, 2956, 2916, 1738, 1649, 1500, 1438, 1373, 1304, 1214, 1163, 1142, 1058, 1021, 929, 919, 811, 789 cm^{-1}. MS, *m/z* (%): 241.0 (100, M + Na). HRMS (ESI+) *m/z*: [M + Na]$^+$ Calcd for $C_9H_{11}ClO_4Na^+$ 241.0238; Found 241.0239. Anal. Calcd. for $C_9H_{11}ClO_4$: C, 49.44; H, 5.07. Found: C, 49.38; H, 5.00. (lit.27)

Dimethyl (*1RS, 2rs, 3SR, 4sr*)-2,4-Dichlorobicyclo[1.1.1]pentane-1,3-dicarboxylate (**9a**). To a solution of **10z** (220 mg, 0.765 mmol) in benzene-d_6 (15 mL) was added TMS_3SiH (283 µL, 0.918 mmol, 1.2 equiv.) and AIBN (31 mg, 0.191 mmol, 25mol%) at room temperature. The clear colorless reaction mixture was stirred 12 h at 80 °C and 14 h at 60 °C. Progress of the reaction was monitored by ^{1}H NMR (500 µL of the reaction mixture was injected into an NMR tube and directly measured; the analyzed sample was returned into the reaction mixture). Volatiles were removed under reduced pressure and column chromatography of the yellow residue on silica gel (hexane/ethyl acetate - 8:1) gave **9a** as a clear colorless oil, which slowly crystallized (167 mg, 0.660 mmol, 86%).

Mp 63.2 - 64.8 °C. ^{1}H NMR (400 MHz, $CDCl_3$): δ 2.20 (dd, J_1 = 4.1 Hz, J_2 = 7.5 Hz, 1H), 3.39 (d, J = 4.1 Hz, 1H), 3.78 (s, 6H), 4.67 (s, 1H), 5.22 (d, J = 7.5 Hz, 1H). ^{13}C {^{1}H} NMR (100 MHz, $CDCl_3$): δ 44.5, 50.0, 52.5, 65.9, 69.2, 164.4. IR (KBr): 3027, 3007, 2956, 2858, 1738, 1439, 1387, 1307, 1296, 1213, 1186, 1170, 1136, 1117, 1104, 1085, 1077, 1036, 1010, 959, 938, 922, 891, 876, 831, 804, 794, 767, 735, 723, 707, 566, 528 cm^{-1}. MS, *m/z* (%): 275.0 (100, M + Na). HRMS (ESI+) *m/z*: [M + Na]$^+$ Calcd for $C_9H_{10}Cl_2O_4Na^+$ 274.9848; Found 274.9848. Anal. Calcd. for $C_9H_{10}Cl_2O_4$: C, 42.71; H, 3.98. Found: C, 42.74; H, 4.05.

Dimethyl 2,2-Dichlorobicyclo[1.1.1]pentane-1,3-dicarboxylate (**9x**). The published procedure27 was adapted as follows. A 500 mL three-necked round bottom flask was charged with CCl_4 (350 mL) that was then cooled to 0 °C and saturated for 1.5 h with dry chlorine. Subsequently, a solution of **7** (2.202 g, 11.408 mmol) in CCl_4 (20 mL) was added and a clear yellow reaction mixture was irradiated with a 150 W incandescent bulb at 0

- 5 °C for 22 h. Reaction progress was monitored by ^{1}H NMR (400 μL of the reaction mixture was injected into an NMR tube, 100 μL of $CDCl_3$ was added and the sample was immediately analyzed). Excess chlorine was purged by stream of argon (exhaust gas was bubbled through 250 mL of saturated aqueous NaOH) until the yellow color of the reaction mixture almost completely vanished (~20 min). Anhydrous methanol (5 mL) was added and the reaction mixture was stirred at room temperature for 20 min. Solvents were removed under reduced pressure. Column chromatography on silica gel (hexane/ethyl acetate - 3:1) afforded the less polar trichloro derivative **10z** (357 mg, 1.242 mmol, 11%), which was eluted first, and then the expected dichloro derivative **9x** (2.196 g, 8.677 mmol, 76%), both as white crystalline solids.

Mp 39.7 - 41.8 °C (lit. 42.0 - 42.5 °C27). ^{1}H NMR (400 MHz, $CDCl_3$): δ 2.48 (m, 2H), 3.01 (m, 2H), 3.80 (s, 6H). ^{13}C {^{1}H} NMR (100 MHz, $CDCl_3$): δ 49.6, 52.4, 52.7, 91.3, 164.9. IR (KBr): 3040, 3000, 2959, 2902, 2857, 1740, 1602, 1559, 1505, 1440, 1379, 1305, 1208, 1141, 1122, 1086, 1061, 1031, 1014, 960, 929, 859, 815, 801725, 620, 544, 504 cm^{-1}. MS, *m/z* (%): 253.0 (22, center of isotope cluster, M + H), 221.0 (34, center of isotope cluster), 192.0 (17), 185.0 (100), 173.0 (14), 157.0 (13). HRMS (CI) *m/z*: $[M + H]^+$ Calcd for $C_9H_{11}Cl_2O_4^+$ 253.0034; Found 253.0032. Anal. Calcd. for $C_9H_{10}Cl_2O_4$: C, 42.71; H, 3.98. Found: C, 42.78; H, 4.02.

Dimethyl (*1RS*, *3SR*, *4sr*)-2,2,4-Trichlorobicyclo[1.1.1]pentane-1,3-dicarboxylate (**10z**). A high-pressure 200 mL Schlenk flask was charged with dry CCl_4 (150 mL) and the solvent was cooled to 0 - 5 °C. Subsequently, chlorine was bubbled through for 20 min followed by addition of **7** (2.398 g, 12.424 mmol) in CCl_4 (10 mL). A clear brightly yellow reaction mixture was irradiated for 16 h with a 500 W incandescent bulb from a distance of 10 - 15 cm at 60 - 65 °C. Reaction progress was monitored by ^{1}H NMR (400 μL of the reaction mixture was mixed with 100 μL of $CDCl_3$ directly in the NMR tube and immediately analyzed). Volume of the reaction mixture was reduced to ~30 mL by distillation at atmospheric pressure and oil bath temperature of 90 °C. Methanol (10 mL) was then added into the reaction mixture and the solution was refluxed for 30 min. Volatiles were removed under reduced pressure and column chromatography on silica gel (hexane/CH_2Cl_2 - 1:3) afforded **10z** (2.250 g, 7.826 mmol, 63%), and **9x** as a more polar side product (209 mg, 0.826 mmol, 7%), both as a white crystalline solids.

Mp 68.3 - 69.1 °C. ^{1}H NMR (400 MHz, $CDCl_3$): δ 3.17 (dd, J_1 = 4.5 Hz, J_2 = 8.0 Hz, 1H), 3.41 (d, J = 4.5 Hz, 1H), 3.83 (s, 6H), 5.21 (d, J = 8.0 Hz, 1H). ^{13}C {^{1}H} NMR (100 MHz, $CDCl_3$): δ 45.3, 52.8, 58.2, 67.9, 87.5, 162.5. IR (KBr): 3044, 3013, 2960, 2859, 1739, 1480, 1443, 1301, 1206, 1187, 1137, 1099, 1077, 1059, 1010, 977, 952, 929, 918, 889, 815, 790, 751, 718, 597 cm^{-1}. MS, *m/z* (%): 308.9 (100, M + Na). HRMS (ESI+) *m/z*: $[M + Na]^+$ Calcd for $C_9H_9Cl_3O_4Na^+$ 308.9459; Found 308.9457. Anal. Calcd. for $C_9H_9Cl_3O_4$: C, 37.60; H, 3.16. Found: C, 37.50; H, 3.15.

Dimethyl 2,2,4,4-Tetrachlorobicyclo[1.1.1]pentane-1,3-dicarboxylate (**11x**). *CAUTION: Reaction involves manipulation with a highly toxic and corrosive gas under high pressure and should be performed only by trained personnel!* A high-pressure Schlenk flask was charged with a solution of **7** (480 mg, 2.487 mmol) in CCl_4 (4 mL). Subsequently, chlorine (~10 mL) was condensed into the reaction mixture at -78 °C. Cooling was stopped and the clear yellow solution was irradiated with a 500 W incandescent bulb from the distance of 6 - 10 cm for 16 h at 50 °C. Progress of the reaction was monitored by ^{1}H NMR (100 - 200 μL of the reaction mixture was cannulated/sucked into NMR tube immersed in liquid nitrogen. Excess of chlorine was allowed to evaporate and the volume of the solution was adjusted with $CDCl_3$ to ca 500 μL.). Irradiation was stopped and the reaction mixture

was cooled to -50 °C. Cooling was then interrupted, chlorine was allowed to slowly evaporate, and releasing gas was trapped in saturated aqueous NaOH (400 mL). Remaining chlorine was purged by stream of argon at room temperature for 5 min. Methanol (8 mL) was then added and the reaction mixture was stirred at the same temperature for additional 15 min. Solvents were removed under reduced pressure and column chromatography on silica gel (hexane/ethyl acetate - 3:1) yielded **11x** as a clear colorless oil that slowly solidified (595 mg, 1.848 mmol, 74%).

Mp 55.1 - 56.4 °C. ^{1}H NMR (400 MHz, $CDCl_3$): δ 3.47 (s, 2H), 3.91 (s, 6H). ^{13}C {^{1}H} NMR (100 MHz, $CDCl_3$): δ 49.0, 53.1, 64.4, 86.8, 160.9. IR (KBr): 3023, 2961, 2903, 2857, 1744, 1700, 1476, 1439, 1385, 1307, 1199, 1170, 1099, 1083, 1036, 1014, 981, 935, 926, 837, 823, 808, 800, 746, 663, 613, 511, 490 cm^{-1}. MS, *m/z* (%): 344.9 (100, centre of isotope cluster, M + Na). HRMS (EI) *m/z*: [M^+] Calcd for $C_9H_8Cl_4O_4^+$ 319.9177; Found 319.9182. Anal. Calcd. for $C_9H_8Cl_4O_4$: C, 33.57; H, 2.50. Found: C, 33.49; H, 2.38.

Hydrolysis of 9 with NaOH in Water. Diester **9x** (2.196 g, 8.677 mmol) was suspended in aqueous NaOH (2.000 g, 50.000 mmol in 50 mL). The white suspension was intensely stirred 5 h at 50 °C. The solid slowly dissolved leaving a brownish solution. The reaction mixture was cooled to room temperature and washed with $CHCl_3$ (3 × 30 mL). The brownish aqueous phase was acidified using concentrated aqueous HCl to pH ~1, and extracted with ether (5 × 25 mL). The clear yellowish organic phase was dried over Na_2SO_4 and solvent was removed under reduced pressure. The yellowish solid residue was dissolved in a minimal amount of ether and **2x** was precipitated with pentane in form of a white crystalline solid (1.080 g, 4.799 mmol, 55%). Analytical sample was obtained by recrystallization from $CHCl_3$.

The yellowish organic phase obtained after precipitation of **2x** was treated at room temperature with ethereal CH_2N_2 until evolution of gas stopped and the organic phase remained permanently yellow. Solvents were removed under reduced pressure and column chromatography on silica gel (hexane/ethyl acetate - 5:2) afforded **13** as a clear slightly yellowish oil (365 mg, 1.556 mmol, 18% based on **9x**).

Dimethyl 2-Chloro-3-(hydroxymethyl)cyclobut-1-ene-1,3-dicarboxylate (**13**). ^{1}H NMR (500 MHz, $CDCl_3$): δ 2.90 (ddd, J_1 = 18.3 Hz, J_2 = 2.1 Hz, J_3 = 1.0 Hz, 1H), 2.91 (ddd, J_1 = 17.0 Hz, J_2 = 2.0 Hz, J_3 = 1.0 Hz, 1H), 3.25 (ddd, J_1 = 17.0 Hz, J_2 = 2.1 Hz, J_3 = 1.6 Hz, 1H), 3.35 (ddd, J_1 = 18.3 Hz, J_2 = 2.1 Hz, J_3 = 1.5 Hz, 1H), 3.78 (s, 3H), 3.84 (s, 3H). ^{13}C {^{1}H} NMR (125 MHz, $CDCl_3$): δ 46.2, 51.4, 52.6, 53.0, 76.3, 124.9, 138.9, 163.0, 174.9. IR (KBr): 3477, 3002, 2956, 2848, 1730, 1631, 1439, 1344, 1284, 1246, 1217, 1072, 1053, 1003, 955, 901, 816, 764 cm^{-1}. GC-MS, *m/z* (%): 235 (2, M + H), 216 (41, M - H_2O), 203 (6, M - OCH_3), 185 (16), 175 (18), 157 (12), 146 (13), 139 (53), 127 (22), 115 (73), 111 (55), 87 (44), 77 (33), 59 (100, $COOCH_3$), 53 (24). HRMS (ESI+) *m/z*: [M + Na]$^+$ Calcd for $C_9H_{11}ClO_5Na^+$ 257.0187; Found 257.0187.

ASSOCIATED CONTENT

Supporting Information

Copies of ^{1}H and ^{13}C NMR spectra of all new compounds, CIFs and ORTEP views of a single molecule and packing in **1**, **2x**, **3z**, **4x**, **9a**, **9x**, and **10z**, optimized geometries of all chlorinated bicyclo[1.1.1]pentanes and parent **0** that were used for computation of the strain energies and pK_a values, and geometries and energies of all structures used in Schemes 6, 7 and 8.

AUTHOR INFORMATION

Corresponding Author
* kaleta@uochb.cas.cz
ORCID
J. Kaleta: 0000-0002-5561-7580
I. Císařová: 0000-0002-9612-9831
M. Dračínský: 0000-0002-4495-0070
J. Michl: 0000-0002-4707-8230
V. Kašička: 0000-0003-1719-1432
V. Šolínová: 0000-0003-0379-8428

Notes
The authors declare no competing financial interest.

ACKNOWLEDGEMENTS

Acknowledgment is made to the Donors of the American Chemical Society Petroleum Research Fund for partial support of this research under award PRF 56668-ND4. This work was also supported by the Institute of Organic Chemistry and Biochemistry, Academy of Sciences of the Czech Republic (RVO: 61388963), Czech Science Foundation (grant no. 17-10832S), and the grant MOBILITY 7AMB (7AMB16FR038). Access to computing and storage facilities owned by parties and projects contributing to the National Grid Infrastructure MetaCentrum provided under the programme „Projects of Large Research, Development, and Innovations Infrastructures“ (CESNET LM2015042), is greatly appreciated. We are grateful to Dr. Lucie Bednárová for help with IR spectra, Prof. Lubomír Pospíšil for preliminary pK_a measurements, and Dr. Jacek Pecyna for performing preliminary experiments.

REFERENCES

1. Levin, M. D.; Kaszynski, P.; Michl, J. Bicyclo[1.1.1]pentanes, [*n*]Staffanes, [1.1.1]Propellanes, and Tricyclo[2.1.0.0^{2,5}]pentanes. *Chem. Rev.* **2000**, *100*, 169-234.

2. Schwab, P. F. H.; Levin, M. D.; Michl, J. Molecular rods. 1. Simple axial rods. *Chem. Rev.* **1999**, *99*, 1863-1933.

3. Dilmac, A. M.; Spuling, E.; de Meijere, A.; Bräse, S. Propellanes - From a Chemical Curiosity to “Explosive” Materials and Natural Products. *Angew. Chem. Int. Ed.* **2017**, *56*, 5684-5718.

4. Makarov, I. S.; Brocklehurst, C.; Kharaghiosoff, K.; Koch, G.; Knochel, P. Synthesis of Bicyclo[1.1.1]pentane Bioisosteres of Internal Alkynes and *para*-Disubstituted Benzenes from [1.1.1]Propellane. *Angew. Chem. Int. Ed.* **2017**, *56*, 12774-12777.

5. Kaleta, J.; Nečas, M.; Mazal, C. 1,3-Diethynylbicyclo[1.1.1]pentane, a Useful Molecular Building Block. *Eur. J. Org. Chem.* **2012**, *25*, 4783-4796.

6. Lemouchi, C.; Iliopoulos, K.; Zorina, L.; Simonov, S.; Wzietek, P.; Cauchy, T.; Fortea, A.; Canadell, E.; Kaleta, J.; Michl, J.; Gindre, D.; Chrysos, M.; Batail, P. Crystalline Arrays of Pairs of Molecular Rotors: Correlated Motion, Rotational

Barriers, and Space-Inversion Symmetry Breaking Due to Conformational Mutations. *J. Am. Chem. Soc.* **2013**, *135*, 9366-9376.

7. Zhao, K.; Dron, P. I.; Kaleta, J.; Rogers, C. T.; Michl, J. Arrays of Dipolar Molecular Rotors in Tris(*o*-phenylenedioxy)cyclotriphosphazene. *Top. Curr. Chem.* **2014**, *354*, 163-212.

8. Kaleta, J.; Janoušek, Z.; Nečas, M.; Mazal, C. Molecular Rods Combining *o*-Carborane and Bicyclo[1.1.1]pentane Cages: An Insertion of the Triple Bond Located Next to a Highly Strained Cage *Organometallics* **2015**, *34*, 967-972.

9. Cipolloni, M.; Kaleta, J.; Mašát, M.; Dron, P. I.; Shen, Y.; Zhao, K.; Rogers, C. T.; Shoemaker, R. K.; Michl, J. Time-Resolved Fluorescence Anisotropy of Bicyclo[1.1.1]pentane/Tolane-Based Molecular Rods Included in Tris(*o*-phenylenedioxy)cyclotriphosphazene (TPP). *J. Phys. Chem. C* **2015**, *119*, 8805-8820.

10. Kaleta, J.; Dron, P. I.; Zhao, K.; Shen, Y.; Císařová, I.; Rogers, C. T.; Michl, J. Arrays of Molecular Rotors with Triptycene Stoppers: Surface Inclusion in Hexagonal Tris(*o*-phenylenedioxy)cyclotriphosphazene. *J. Org. Chem.* **2015**, *80*, 6173-6192.

11. Kaleta, J.; Michl, J.; Mézière, C.; Simonov, S.; Zorina, L.; Wzietek, P.; Rodríguez-Fortea, A.; Canadell, E.; Batail, P. Gearing Motion in Cogwheel Pairs of Molecular Rotors: Weak-Coupling Limit. *CrystEngComm* **2015**, *17*, 7829-7834.

12. Dron, P. I.; Zhao, K.; Kaleta, J.; Shen, Y.; Wen, J.; Shoemaker, R. K.; Rogers, C. T.; Michl, J. Bulk Inclusions of Pyridazine Based Molecular Rotors in Tris(*o*-phenylenedioxy)cyclotriphosphazene (TPP). *Adv. Funct. Mater.* **2016**, *26*, 5718-5732.

13. Kaleta, J.; Chen, J.; Bastien, G.; Dračínský, M.; Mašát, M.; Rogers, C. T.; Feringa, B. L.; Michl, J. Surface Inclusion of Unidirectional Molecular Motors in Hexagonal Tris(*o*-phenylene)cyclotriphosphazene. *J. Am. Chem. Soc.* **2017**, *139*, 10486-10498.

14. Rodríguez-Fortea, A.; Kaleta, J.; Mézière, C.; Allain, M.; Canadell, E.; Wzietek, P.; Michl, J.; Batail, P. Asymmetric Choreography in Pairs of Orthogonal Rotors. *ACS Omega* **2018**, *3*, 1293-1297.

15. Kaleta, J.; Bastien, G.; Císařová, I.; Batail, P.; Michl, J. Molecular Rods: Facile Desymmetrization of 1,4-Diethynylbicyclo[2.2.2]octane. *Eur. J. Org. Chem.* **2018**, *37*, 5137-5142.

16. Pellicciari, R.; Raimondo, M.; Marinozzi, M.; Natalini, B.; Costantino, G.; Thomsen, C. (S)-(+)-2-(3′-Carboxybicyclo[1.1.1]pentyl)glycine, a Structurally New Group I Metabotropic Glutamate Receptor Antagonist. *J. Med. Chem.* **1996**, *39*, 2874-2876.

17. Thirumoorthi, N. T.; Shen, C. J.; Adsool, V. A. Expedient Synthesis of 3-Phenylbicyclo[1.1.1]pentan-1-amine *via* Metal-Free Homolytic Aromatic Alkylation of Benzene. *Chem. Commun.* **2015**, *51*, 3139-3142.

18. Gianatassio, R.; Lopchuk, J. M.; Wang, J.; Pan, C.-M.; Malins, L. R.; Prieto, L.; Brandt, T. A.; Collins, M. R.; Gallego, G. M.; Sach, N. W.; Spangler, J. E.; Zhu, H.; Zhu, J.; Baran, P. S. Strain-Release Amination. *Science* **2016**, *351*, 241-246.

19. Lopchuk, J. M.; Fjelbye, K.; Kawamata, Y.; Malins, L. R.; Pan, C.-M.; Gianatassio, R.; Wang, J.; Prieto, L.; Bradow, J.; Brandt, T. A.; Collins, M. R.; Elleraas, J.; Ewanicki, J.; Farrell, W.; Fadeyi, O. O.; Gallego, G. M.; Mousseau, J. J.; Oliver, R.; Sach, N. W.; Smith, J. K.; Spangler, J. E.; Zhu, H.; Zhu, J.; Baran, P. S. Strain-Release Heteroatom Functionalization: Development, Scope, and Stereospecificity. *J. Am. Chem. Soc.* **2017**, *139*, 3209-3226.

20. Pellicciari, R.; Filosa, R.; Fulco, M. C.; Marinozzi, M.; Macchiarulo, A.; Novak, C.; Natalini, B.; Hermit, M. B.; Nielsen, S.; Sager, T. N.; Stensbol, T. B.; Thomsen, C. Synthesis and Preliminary Biological Evaluation of 2'-Substituted 2-(3'-Carboxybicyclo[1.1.1]pentyl)glycine Derivatives as Group I Selective Metabotropic Glutamate Receptor Ligands. *ChemMedChem.* **2006**, *1*, 358-365.

21. Kanazawa, J.; Maeda, K.; Uchiyama, M.. Radical Multicomponent Carboamination of [1.1.1]Propellane. *J. Am. Chem. Soc.* **2017**, *139*, 17791-17794.

22. Caputo, D. F. J.; Arroniz, C.; Dürr, A. B.; Mousseau, J. J.; Stepan, A. F.; Mansfeld, S. J.; Anderson, E. A. Synthesis and Applications of Highly Functionalized 1-halo-3-substituted bicyclo[1.1.1]pentanes. *Chem. Sci.* **2018**, *9*, 5295-5300.

23. Mikhailiuk, P. V.; Afonin, S.; Chernega, A. N.; Rusanov, E. B.; Platonov, M. O.; Dubinina, G. D.; Berditsch, M.; Ulrich, A. S.; Komarov, I. V. Conformationally Rigid Trifluoromethyl-Substituted α-Amino Acid Designed for Peptide Structure Analysis by Solid-State ^{19}F NMR Spectroscopy. *Angew. Chem. Int. Ed.* **2006**, *45*, 5659-5661.

24. Stulgies, B.; Pigg, D. P.; Kaszynski, P.; Kudzin, Z. H. 9,9-Dimethyl-8,10-dioxapentacyclo[5.3.0.0^{2,5}.0^{3,5}.0^{3,6}]decane and naphthotetracyclo[5.1.0.0^{1,6}.0^{2,7}]oct-3-ene: New Substituted [1.1.1]propellanes as Precursors to 1,2,3,4-tetrafunctionalized bicyclo[1.1.1]pentanes. *Tetrahedron* **2005**, *61*, 89-95.

25. Mazal, C.; Škarka, O.; Kaleta, J.; Michl, J. *cis-endo*-Bicyclo[1.1.1]pentane-1,2,3,4-tetracarboxylic Acid and Its Derivatives. *Org. Lett.* **2006**, *8*, 749-752.

26. Kaleta, J.; Michl, J.; Mazal, C. T-Shaped Molecular Building Blocks by Combined Bridgehead and Bridge Substitution on Bicyclo[1.1.1]pentanes. *J. Org. Chem.* **2010**, *75*, 2350-2356.

27. Robinson, R.; Michl, J. Chlorination of bicyclo[1.1.1]pentane derivatives. *J. Org. Chem.* **1989**, *54*, 2051-2053.

28. Hall, H. K.; Smith, C. D.; Blanchard, E. P.; Cherkofsky, S. C.; Sieja, J. B. Synthesis and Polymerization of Bridgehead-Substituted Bicyclobutanes. *J. Am. Chem. Soc.* **1971**, *93*, 121-130.

29. Applequist, D. E.; Renken, T. L.; Wheeler, J. W. Polar Substituent Effects in 1,3-Disubstituted bicyclo[1.1.1]pentanes. *J. Org. Chem.* **1982**, *47*, 4985-4995.

30. Wiberg, K. B.; Dailey, W. P.; Walker, F. H.; Waddell, S. T.; Crocker, L. S.; Newton, M. Vibrational Spectrum, Structure, and Energy of [1.1.1]propellane. *J. Am. Chem. Soc.* **1985**, *107*, 7247-7257.

31. Shtarev, A. B.; Pinkhassik, E.; Levin, M. D.; Stibor, I.; Michl, J. Partially Bridge-Fluorinated Dimethyl Bicyclo[1.1.1]pentane-1,3-dicarboxylates: Preparation and NMR Spectra. *J. Am. Chem. Soc.* **2001**, *123*, 3484-3492.

32. Levin, M. D.; Hamrock, S. J.; Kaszynski, P.; Shtarev, A. B.; Levina, G. A.; Noll, B. C.; Ashley, M. E.; Newmark, R.; Moore, G. G. I.; Michl, J. Preparation, Structure, and Properties of Symmetrically 1,3-Difunctionalized Penta- and Hexafluorobicyclo-[1.1.1]pentanes. *J. Am. Chem. Soc.* **1997**, *119*, 12750-12761.

33. Balaji, V.; Michl, J. New Strained Organic Molecules: Theory Guides Experiment. New Strained Organic Molecules: Theory Guides Experiment. *Pure Appl. Chem.* **1988**, *60*, 189.

34. Kaszynski, P.; Michl, J. Heterogeneous Acid-Catalyzed Amination of Isobutene to *tert*-butylamine. *J. Org. Chem.* **1988**, *53*, 4594-4596.

35. Wheeler, E. S.; Houk, N. K.; Schleyer, v. R. P.; Allen, D. W. A Hierarchy of Homodesmotic Reactions for Thermochemistry. *J. Am. Chem. Soc.* **2009**, *131*, 2547-2560.

36. Šolínová, V.; Kašička, V. Determination of Acidity Constants and Ionic Mobilities of Polyprotic Peptide Hormones by CZE. *Electrophoresis* **2013**, *34*, 2655-2665.

37. Alabugin, I. V. *Stereoelectronic Effects: The Bridge between Structure and Reactivity*; John Wiley & Sons Ltd, 2016.

38. Wiberg, K. B. The Concept of Strain in Organic Chemistry. *Angew. Chem., Int. Ed. Engl.* **1986**, *25*, 312-322.

39. Cottrell, T. L. *The Strengths of Chemical Bonds,* 2d ed., Butterworth, London, 1958.

40. Yue, Z.; Haiyan, Q.; Xianglan, C.; Zelin, L.; Shangci, Y.; Xiaoming, X. Thermodynamic Estimate of pK_a Values of the Carboxylic Acids in Aqueous Solution with the Density Functional Theory. *Chin. J. Chem.* **2010**, *28*, 727-733.

41. Sheldrick, G. M. *SHELXT* - Integrated Space-Group and Crystal-Structure Determination. *Acta Cryst.* **2015**, *A71*, 3-8.

42. Sheldrick, G. M. Crystal Structure Refinement With *SHELXL*. *Acta Cryst.* **2015**, *C71*, 3-8.

43. Tan, B.; Long, X.; Li, J. Theoretical Investigation of Several 1,2,3,4-Tetrazine Based High Energy Compounds. *Comp. Theor. Chem.* **2012**, *993*, 66-72.

44. Pan, Y.; Zhu, W.; Xiao, H. Theoretical Studies of a Series of Azaoxaisowurtzitane Cage Compounds with High Explosive Performance and Low Sensitivity. *Comp. Theor. Chem.* **2017**, *1114*, 77-86.

45. Sellers, D. B.; James, C. N.; Gobbi, A. A Comparison of Quantum and Molecular Mechanical Methods to Estimate Strain Energy in Druglike Fragments. *J. Chem. Inf. Model.* **2017**, *57*, 1265-1275.

46. Pan, Y.; Zhu, W. Designing and Looking for Novel Cage Compounds Based on Bicyclo-HMX as High Energy Density Compounds. *RSC Adv.* **2018**, *8*, 44-52.

47. Grimme, S.; Ehrlich, S.; Goerigk, L. Effect of the Damping Function in Dispersion Corrected Density Functional Theory. *J. Comp. Chem.* **2011**, *32*, 1456-1465.

48. Marenich, V. A.; Cramer, J. C.; Truhlar, G. D. Universal Solvation Model Based on Solute Electron Density and on a Continuum Model of the Solvent Defined by the Bulk Dielectric Constant and Atomic Surface Tensions. *J. Phys. Chem. B* **2009**, *113*, 6378-6396.

49. Pliego, J. R.; Riveros, J. M. The Cluster-Continuum Model for the Calculation of the Solvation Free Energy of Ionic Species. *J. Phys. Chem. A* **2001**, *105*, 7241-7247.

50. Seybold, G. P.; Shields, C. G. Computational Estimation of pK_a Values. *WIREs Comput. Mol. Sci.* **2015**, *5*, 290-297.

51. Gaussian 09, Revision B.01, Frisch, M. J.; Trucks, G. W.; Schlegel, H. B.; Scuseria, G. E.; Robb, M. A.; Cheeseman, J. R.; Scalmani, G.; Barone, V.; Mennucci, B.; Petersson, G. A.; Nakatsuji, H.; Caricato, M.; Li, X.; Hratchian, H. P.; Izmaylov, A. F.; Bloino, J.; Zheng, G.; Sonnenberg, J. L.; Hada, M.; Ehara, M.; Toyota, K.; Fukuda, R.; Hasegawa, J.; Ishida, M.; Nakajima, T.; Honda, Y.; Kitao, O.; Nakai, H.; Vreven, T.; Montgomery, J. A., Jr.; Peralta, J. E.; Ogliaro, F.; Bearpark, M.; Heyd, J. J.; Brothers, E.; Kudin, K. N.; Staroverov, V. N.; Kobayashi, R.; Normand, J.; Raghavachari, K.; Rendell, A.; Burant, J. C.; Iyengar, S. S.; Tomasi, J.; Cossi, M.; Rega, N.; Millam, J. M.; Klene, M.; Knox, J. E.; Cross, J. B.; Bakken, V.; Adamo, C.; Jaramillo, J.; Gomperts, R.; Stratmann, R. E.; Yazyev, O.; Austin, A. J.; Cammi, R.; Pomelli, C.; Ochterski, J. W.; Martin, R. L.; Morokuma, K.; Zakrzewski, V. G.; Voth, G. A.; Salvador, P.; Dannenberg, J. J.; Dapprich, S.; Daniels, A. D.; Farkas, Ö.; Foresman, J. B.; Ortiz, J. V.; Cioslowski, J.; Fox, D. J. Gaussian, Inc., Wallingford CT, 2009.

52. Barone, V.; Cossi, M. Quantum Calculation of Molecular Energies and Energy Gradients in Solution by a Conductor Solvent Model. *J. Phys. Chem. A* **1998**, *102*, 1995-2001.

53. Cossi, M.; Rega, N.; Scalmani, G.; Barone, V. Energies, Structures, and Electronic

Properties of Molecules in Solution With the C PCM Solvation Model. *J. Comput. Chem.* **2003**, *24*, 669-681.

54. Frisch, M. J.; Trucks, G. W.; Schlegel, H. B.; Scuseria, G. E.; Robb, M. A.; Cheeseman, J. R.; Scalmani, G.; Barone, V.; Petersson, G. A.; Nakatsuji, H.; Li, X.; Caricato, X.; Marenich, A. V.; Bloino, J.; Janesko, B. G.; Gomperts, R.; Mennucci, B.; Hratchian, H. P.; Ortiz, J. V.; Izmaylov, A. F.; Sonnenberg, J. L.; Williams-Young, D.; Ding, F.; Lipparini, F.; Egidi, F.; Goings, J.; Peng, B.; Petrone, A.; T. Henderson; D. Ranasinghe; V. G. Zakrzewski; J. Gao; N. Rega; G. Zheng; W. Liang; M. Hada; M. Ehara; K. Toyota; R. Fukuda; J. Hasegawa; M. Ishida; T. Nakajima; Y. Honda; O. Kitao; H. Nakai; T. Vreven; K. Throssell; Montgomery, J., J. A. ; Peralta, J. E.; Ogliaro, F.; Bearpark, M. J.; Heyd, J. J.; Brothers, E. N.; Kudin, K. N.; Staroverov, V. N.; Keith, T. A.; Kobayashi, R.; Normand, J.; Raghavachari, K.; Rendell, A. P.; Burant, J. C.; Iyengar, S. S.; Tomasi, J.; Cossi, M.; Millam, J. M.; Klene, M.; Adamo, C.; Cammi, R.; Ochterski, J. W.; Martin, R. L.; Morokuma, K.; Farkas, O.; Foresman, J. B.; Fox, D. J. *Gaussian 16, Revision A.03*, Gaussian, Inc.: Wallingford CT, 2016.